

University of Louisville

ThinkIR: The University of Louisville's Institutional Repository

Electronic Theses and Dissertations

1-2018

Detection of trace tetrahydrocannabinol (THC) through surface enhanced Raman spectroscopy (SERS) on microfabricated platforms

Jack T Lockard
University of Louisville

Follow this and additional works at: <https://ir.library.louisville.edu/etd>



Part of the [Engineering Commons](#)

Recommended Citation

Lockard, Jack T, "Detection of trace tetrahydrocannabinol (THC) through surface enhanced Raman spectroscopy (SERS) on microfabricated platforms" (2018). *Electronic Theses and Dissertations*. Paper 3454.

<https://doi.org/10.18297/etd/3454>

This Master's Thesis is brought to you for free and open access by ThinkIR: The University of Louisville's Institutional Repository. It has been accepted for inclusion in Electronic Theses and Dissertations by an authorized administrator of ThinkIR: The University of Louisville's Institutional Repository. This title appears here courtesy of the author, who has retained all other copyrights. For more information, please contact thinkir@louisville.edu.

DETECTION OF TRACE TETRAHYDROCANNABINOL (THC) THROUGH SURFACE
ENHANCED RAMAN SPECTROSCOPY (SERS) ON MICROFABRICATED PLATFORMS

By

Jack Lockard
B.S., University of Louisville, 2017

A Thesis
Submitted to the Faculty of the
University of Louisville
J.B. Speed School of Engineering
As Partial Fulfillment of the Requirements
For the Professional Degree

MASTER OF ENGINEERING

Department of Chemical Engineering

December 2018

DETECTION OF TRACE TETRAHYDROCANNABINOL (THC) THROUGH SURFACE
ENHANCED RAMAN SPECTROSCOPY (SERS) ON MICROFABRICATED PLATFORMS

Submitted by: 
Jack Lockard

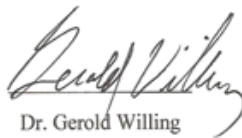
A Thesis Approved On

11/28/18
(Date)

By the Following Reading and Examination Committee



Dr. Xiao-An Fu, Thesis Director


Dr. Gerold Willing
Dr. Gamini Sumanasekera

ACKNOWLEDGMENTS

I would like to thank my thesis adviser, Dr. Xiao-An Fu, for sparking my interest in microsystems and guiding me through my first foray into research. I would like to thank the other members of the committee; Dr. Gerold Willing, who over the years has proven to be a great and reliable professor; and Dr. Gamini Sumanasekera for his willingness to be a member on my thesis committee.

I would like to thank the staff of the University of Louisville Micro/Nano Technology Center for their training and expertise on the equipment used in these experiments. In particular, thank you to Dr. Julia Aebersold and Curt McKenna for their assistance and willingness to answer any of my questions.

I would also like to thank doctoral candidate Qi Li and Dr. Zhenzhen Xie for their assistance in this work. A big thank you to Dr. Zhenzhen, who was crucial in collecting data for the final steps of the research.

ABSTRACT

As an increasing number of states legalize marijuana, it will become necessary to create a method for portable detection and quantification of tetrahydrocannabinol (THC), the principal psychoactive component of cannabis. The ability to identify impaired individuals without the need for traditional drug testing could prove invaluable to law enforcement and employers. Toward this end goal, surface enhanced Raman spectroscopy (SERS) with a silver treated, silicon nanowire substrate was investigated as a method for detection.

Acid wet etching of silicon with a hydrofluoric acid (HF) / silver nitrate (AgNO_3) was the primary investigation method for this work. Various etching parameters were utilized, ranging from 2 M HF/0.02 M AgNO_3 , 5 M HF/0.02 M AgNO_3 , 5 M HF/0.10 M AgNO_3 , 8.15 M HF/0.02 M AgNO_3 , to 12.2 M HF/0.02 M AgNO_3 . Bare, unetched silicon and silver sputtered silicon were tested as substrates for SERS for THC detection, but proved to have no signal enhancement. Nanowires were not present at 2 M HF/0.02 M AgNO_3 etching conditions and the substrate provided no Raman enhancement. Residual silver from the wet etching was tested to see if it was a viable means of enhancing Raman signal. Measurements spanning from 5 M HF/0.02 M AgNO_3 to 12.2 M HF/0.02 M AgNO_3 indicate residual silver can be used to enhance signal, but its sparse and irregular distribution over the silicon nanowire substrate leads to inconsistent measurements that require aiming the laser at residual silver deposits. The increased AgNO_3 etching parameters (5 M HF/0.10 M AgNO_3) yielded a residual silver particle film which obstructed the silicon nanowires. The resulting lack of Raman signal enhancement indicated nanowires were necessary in addition to silver for SERS activity. Etching parameters of 8.15 M HF/0.02 M AgNO_3 and 12.2 M HF/0.02 M AgNO_3 both displayed Raman activity at 1.0×10^7 pg of THC on sputtered chips,

and at 3.15 pg on chips with residual silver. The 1.0×10^7 pg of THC tests were performed to determine if the chips could detect a relatively large amount of THC, while the 3.15 pg THC tests were performed to determine if the method could detect THC on the order of magnitude present in breath. The Raman response displayed by the tests indicated qualitative detection is possible. Quantitative tests with THC amounts ranging from 2.4 pg to 10,005.6 pg on the 8.15 M HF/0.02 M AgNO₃ (chosen due to its larger signal intensity compared to the other trial conditions) chip indicate reliable quantitative analysis was not possible with these conditions and should be the subject of future works.

TABLE OF CONTENTS

I.	INTRODUCTION.....	1
II.	REVIEW OF LITERATURE.....	4
A.	CHEMISTRY OF THC IN THE BODY.....	4
B.	SERS, WHAT IT IS AND HOW IT WORKS.....	6
C.	SERS FOR THC/DRUG DETECTION.....	7
D.	THC DETECTION IN GAS PHASE/EXHALED BREATH.....	8
E.	MICROPILLARS AS SERS SUBSTRATE.....	10
F.	DRY ETCHING.....	11
G.	WET ETCHING.....	15
H.	DRY ETCHING VERSUS WET ETCHING.....	17
III.	EXPERIMENTAL.....	18
A.	EXPERIMENTAL PLAN.....	18
B.	MATERIALS.....	19
C.	EQUIPMENT.....	20
D.	EXPERIMENTAL PROCEDURES.....	23
IV.	RESULTS AND DISCUSSION.....	31
A.	PHOTOLITHOGRAPHY.....	31
B.	WET ETCHING MORPHOLOGY.....	35
C.	SPUTTERING OF SILVER.....	61
D.	RAMAN SPECTROSCOPY RESULTS.....	63
V.	CONCLUSION.....	81
VI.	RECOMMENDATIONS.....	83
	REFERENCES.....	84
	VITA.....	87

LIST OF TABLES

Table 1 Summary of THC Detection Research	10
Table 2: Optimized Sputtering Conditions	26
Table 3: Trial 1 and Trial 2 Etch Parameters.....	35
Table 4: Trial 4 through 6 Parameters	40
Table 5: Trial 7 through 9 Parameters	43
Table 6: Trial 10 through 13 Parameters	49
Table 7: Intensity at 1390 cm^{-1} for Varying Amounts of THC (for Figure 72).....	78
Table 8: Intensity at 1390 cm^{-1} for Varying Amounts of THC (for Figure 74).....	80

LIST OF FIGURES

Figure 1: Marijuana Legalization status as of December 2018 [Governing.com, 2018].....	2
FIGURE 2-Tetrahydrocannabinol (THC) [Pubchem, 2018]	4
FIGURE 3- Primary metabolite 11-OH-THC [Pubchem, 2018]	
FIGURE 4- Secondary metabolite THC-COOH [Pubchem, 2018].....	4
Figure 5: Conceptual Illustration of SERS [Semrock.com, 2018]	6
Figure 6- Polyimide Method: a) PI spun on; b) Plasma treating PI; c) Plasma etching; d) Wet etching; e) Metal deposition [Li et al., 2017]	12
Figure 7- Morphology of Polyimide Method [Li et al., 2017].....	12
Figure 8- a) Variation of profile angle with etching and passivation times at 600 W and 12 W platen power. b) Profile angle at different etch to passivation cycle times with varying platen power at 600 W coil power. [Miller et al., 2012].....	13
Figure 9- Silicon micropillars fabricated by DRIE exhibiting a) positive ($>90^\circ$), b) negative ($<90^\circ$) and c) near 90° profiles. [Miller et al., 2012]	14
Figure 10- Schematic for the synthesis of Ag-NP@Ge-nanotapers/Si-micropillar hierarchical arrays. [Liu et al., 2015]	15
Figure 11: HF/AGNO ₃ Etchant Mechanism (Srivastava et al, 2014).....	16
Figure 12- a) SEM cross-section image of silicon nanowire arrays. b) TEM image of an individual SiNW prepared from a p-type (111)-oriented silicon substrate. c) HRTEM image of the nanowire in Figure 1b (the inset is the ED pattern recorded along the [110] axis). d) HRTEM image of a nanowire synthesized from a p-type (100)-oriented silicon substrate (the inset is its ED pattern recorded along the [001] axis). (Peng et al., 2005)	16
Figure 13: Acid Wet Bench.....	21
Figure 14: Lesker PVD 75 Sputterer	21
Figure 15: Scanning Electron Microscope.....	22
Figure 16: Dektak Profilometer.....	22
Figure 17: Raman Spectrometer	23
Figure 18: Photoresist pillars on Si, x5 magnification	31
Figure 19: Photoresist pillars, x20 magnification.....	32
Figure 20: Photoresist pillars, x50 magnification.....	32
Figure 21: Post-etch photoresist pillars on Si, x5 magnification.....	33
Figure 22: Post-etch photoresist pillars on Si, x20 magnification.....	34
Figure 23: Post-etch photoresist pillars on Si, x50 magnification.....	34
Figure 24: Trial 1, 7.14 M HF, 2 hour, 50°C etch from top down view	36
Figure 25: Trial 1, 7.14 M HF, 2 hour, 50°C etch from top down view	37
Figure 26: Trial 1, 7.14 M HF, 2 hour, 50°C etch from top down view	37
Figure 27: Trial 1, dendritic residual silver from top down view	38
Figure 28: Trial 1, residual silver particles from top down view.....	38
Figure 29: Top view of trial 2, 1 hour, 30°C etch	39

Figure 30: Trial 3, 2.00 M HF viewed from top down	41
Figure 31: Trial 5, 5.00 M HF viewed from top down	41
Figure 32: Trial 6, 7.90 M HF viewed from top down	42
Figure 33: Trial 4, 10.40 M HF viewed from top down	42
Figure 34: Trial 7, 2 M HF viewed from 20° tilt	44
Figure 35: Trial 8, 8.15 M HF viewed from top down	45
Figure 36: Trial 8, 8.15 M HF viewed from 20° tilt	45
Figure 37: Trial 8, 8.15 M HF viewed from 20° tilt	46
Figure 38: Trial 9, 12.2 M HF viewed from top down	47
Figure 39: Trial 9, 12.2 M HF viewed from 20° tilt	47
Figure 40: Trial 9, 12.2 M HF viewed from 20° tilt	48
Figure 41: Trial 10, 5 M HF, 0.10 M AgNO ₃ , top down view	49
Figure 42: Trial 10, 5 M HF, 0.10 M AgNO ₃ , top down view	50
Figure 43: Trial 11, 5 M HF, 0.02 M AgNO ₃ , residual silver top down view	51
Figure 44: Trial 11, 5 M HF, 0.02 M AgNO ₃ , residual silver top down view	51
Figure 45: Trial 11, 5 M HF, 0.02 M AgNO ₃ , residual silver top down view	52
Figure 46: Trial 11, 5 M HF, 0.02 M AgNO ₃ , residual silver, 20° tilt view	53
Figure 47: Trial 11, 5 M HF, 0.02 M AgNO ₃ , residual silver, 20° tilt view	53
Figure 48: Trial 12, 8.15 M HF, 0.02 M AgNO ₃ , top down view	54
Figure 49: Trial 12, 8.15 M HF, 0.02 M AgNO ₃ , top down view	55
Figure 50: Trial 12, 8.15 M HF, 0.02 M AgNO ₃ , 20° tilt view	55
Figure 51: Trial 12, 8.15 M HF, 0.02 M AgNO ₃ , 20° tilt view	56
Figure 52: Trial 13, 12.2 M HF, 0.02 M AgNO ₃ , top down view	56
Figure 53: Trial 13, 12.2 M HF, 0.02 M AgNO ₃ , top down view	57
Figure 54: Trial 13, 12.2 M HF, 0.02 M AgNO ₃ , 20° tilt view	57
Figure 55: Trial 7, 2 M HF, 0.02 M AGNO ₃ , sputtered Ag top down view.....	58
Figure 56: Trial 8, 8.15 M HF, 0.02 M AGNO ₃ , sputtered Ag top down view.....	59
Figure 57: Trial 8, 8.15 M HF, 0.02 M AGNO ₃ , sputtered Ag top down view.....	59
Figure 58: Trial 9, 12.2 M HF, 0.02 M AGNO ₃ , sputtered Ag top down view.....	60
Figure 59: Trial 9, 12.2 M HF, 0.02 M AGNO ₃ , sputtered Ag top down view.....	60
Figure 60: Profilometer measurement, 300 W power, 30 minute pump time, 1 minute deposition time	61
Figure 61: Profilometer measurement, 150 W power, 60 minute pump time, 1 minute deposition time	62
Figure 62: Profilometer measurement, 150 W power, 60 minute pump time, 30 second deposition time	63
Figure 63: 10 μ L (1.0*10 ⁷ pg) of THC on bare Si	64
Figure 64: Bare Si chip, 10 μ L (1.0*10 ⁷ pg) of THC on bare Si with Ag sputtered on.....	65
Figure 65: Trial 7 chip, 2 M HF, 0.02 M AgNO ₃ solution, 1006 pg of THC.....	66
Figure 65: Trial 11, 5 M HF, 0.02 M AgNO ₃ , 3.15 pg THC over no residual Ag.....	67
Figure 66: Trial 11, 5 M HF, 0.02 M AgNO ₃ , 3.15 pg THC over residual Ag.....	67
Figure 67: Trial 10, 10 μ L (1.0*10 ⁷ pg) of THC on Si chip etched with 5 M HF/0.10 M AgNO ₃ with residual Ag	69

Figure 65: Trial 8, 10 μL (1.0×10^7 pg) of THC on Si chip etched with 8.15 M HF/0.02 M AgNO_3 with sputtered silver	70
Figure 69: Trial 12, 3.15 pg of THC on Si chip etched with 8.15 M HF/0.02 M AgNO_3 with residual silver, measurement over no silver area on chip	71
Figure 70: Trial 12, 3.15 pg of THC on Si chip etched with 8.15 M HF/0.02 M AgNO_3 with residual silver, measurement over silver on chip	71
Figure 71: Trial 9, 10 μL (1.0×10^7 pg) of THC on Si chip etched with 12.2 M HF/0.02 M AgNO_3 with sputtered silver	73
Figure 72: Trial 13, 3.15 pg of THC on Si chip etched with 12.2 M HF/0.02 M AgNO_3 with residual silver, measurement over no silver area on chip	74
Figure 73: Trial 13, 3.15 pg of THC on Si chip etched with 12.2 M HF/0.02 M AgNO_3 with residual silver, measurement over no silver area on chip	74
Figure 74: Raman response to various amounts of THC using the front part of the data as a baseline	76
Figure 75: Calibration curve from the response intensity at 1390 cm^{-1} from Figure 71	77
Figure 76: Raman response to various amounts of THC using the tail part of the data as a baseline	79
Figure 77: Calibration curve from the response intensity at 1390 cm^{-1} from Figure 73	80

I. INTRODUCTION

Over the past 20 years scientists have been researching and creating more sensitive and effective means of trace chemical detection and analysis. Researchers have created systems which have a limit of detection (LOD) to as low as parts per billion in a sample. An effective method for creation of such systems is microfabrication. There are portable systems capable of detecting pollutants in water (Li et al., 2013) or detecting trace amounts of explosive compounds (Almaviva, Botti, Cantarini et al., 2012). Point of care diagnostic devices for medical care are under development as well (Wlodkowic and Cooper, 2010). Currently, there is a need for a device with similar sensing capabilities able to quickly and accurately detect and quantify tetrahydrocannabinol (THC), the principal psychoactive component of cannabis.

Currently, 33 states have some form of widespread marijuana legality, with 10 states and the District of Columbia having recreational legality. As an increasing number of states legalize marijuana, it is becoming necessary to be able to identify impaired drivers or workers, analogous to the ability of a portable alcohol breathalyzer. A real time analyzer for marijuana would prove invaluable to law enforcement and companies desiring to identify impaired individuals.

The objective of this research is to lay the groundwork for the creation of a “marijuana breathalyzer.” This research focuses on creating a microfabricated chemical sensing platform with the capability of measuring THC concentration. Surface-enhanced Raman spectroscopy (SERS) served as the primary detection method. Photolithography and deep reactive ion etching (DRIE) were explored as a method to create sharp tipped micropillar structures; however, wet chemical etching using a solution of hydrofluoric acid and silver nitrate was ultimately used as the fabrication method. The nanowire structures were coated with silver by a sputtering process to enhance the Raman signal strength. From there, various concentrations of THC in a methanol solution were evaporated on the device chip and Raman spectroscopy was used to analyze the sample. Concentrations near those found in exhaled breath were also created to test the potential of the device working as a breath analysis tool.

II. REVIEW OF LITERATURE

A. CHEMISTRY OF THC IN THE BODY

The work undertaken for the proposed device set out to accomplish the goals of identifying and quantifying the concentration of tetrahydrocannabinol (THC) and associated metabolites, 11-hydroxy-THC (11-OH-THC) and 11-nor-9-carboxy-THC (THC-COOH), in a simulated breath sample.

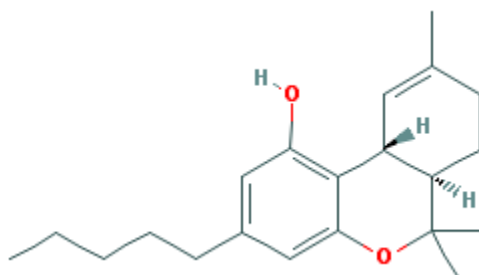


FIGURE 2-Tetrahydrocannabinol (THC) [Pubchem, 2018]

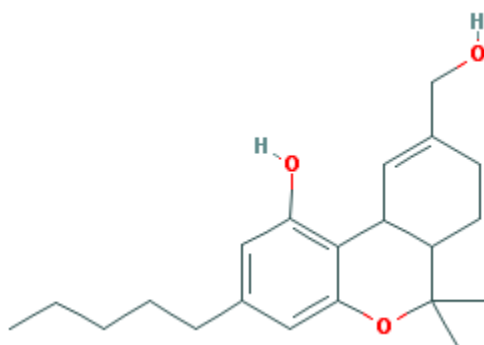


FIGURE 3- Primary metabolite 11-OH-THC [Pubchem, 2018]

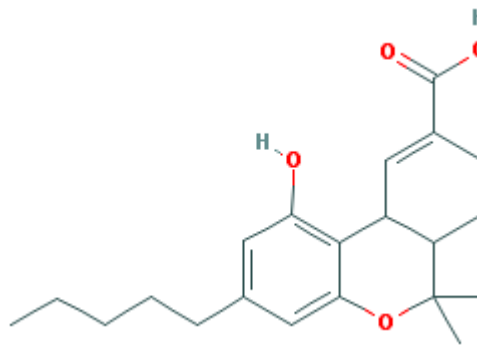


FIGURE 4- Secondary metabolite THC-COOH [Pubchem, 2018]

The primary and secondary metabolites of THC are formed in the body by oxidative metabolism (Huestis et al., 1992). According to the National Institute on Drug Abuse, roughly 80% to 90% of THC is excreted as metabolites within 5 days (1987). Currently in the field of drug testing, THC and associated metabolites are detected in bodily fluids (such as blood and urine) through thin layer chromatography, gas chromatography/mass spectrometry (GC-MS), radioimmunoassay, or enzyme immunoassay. For tests designed to detect any level of THC consumption, the target compound is either unconverted THC or the secondary metabolite THC-COOH due to the comparatively longer amount of time THC-COOH resides in the body (compared to 11-OH-THC). Low levels of THC have been detected for more than 5 weeks in urine and feces. THC is processed in the liver which in turn produces the metabolites.

This proves a design challenge for a breathalyzer-style device in that the markers of THC are mostly present in blood, urine, and fecal matter. Product designers have attempted to overcome this obstacle in the past by using saliva as the analyte (Day, Kuntz, Fieldman, 2010). A small portion of THC-COOH can be detected in saliva and used as a biomarker for the active intake of THC. In this technique, saliva is collected from a swab or by expectorating into a cup. The sample is then analyzed or stored in a preservative solution for off-site analysis. The target metabolite THC-COOH is then extracted from the sample, purified and concentrated using an extraction column, and analyzed using GC-MS.

B. SERS, WHAT IT IS AND HOW IT WORKS

Surface enhanced Raman spectroscopy (SERS) is defined as the signal enhancement in Raman spectroscopy due to Raman scattering and the excitement of the localized surface plasmon resonance. The first observed instance of surface enhancement for Raman spectroscopy occurred in 1974 (Fleischmann, et al.). The researchers utilized electrochemical roughening on metals such as copper and silver to create enhancement of the Raman scattering. This technique resulted in an enhancement factor of 10^6 . The enhancement stems from an electromagnetic enhancement mechanism and the chemical etchant mechanism (Stiles et al., 2008). An electromagnetic wave from a spectrometer interacts with the surface of the metal. A rough metal surface has the potential to excite localized surface plasmons. Localized surface plasmons are the electromagnetic field-driven coherent oscillation of the surface conduction electrons in a material with negative and near-zero imaginary dielectric constants (Stiles et al., 2008). The excitement of the localized surface plasmons results in amplification of the electromagnetic fields at the metal surface. The increased intensity of the electromagnetic fields will then create an enhancement of Raman scattering. Raman scattering is the inelastic scattering of a photon from a molecule in which the frequency change precisely matches the difference in vibrational energy levels (Stiles et al., 2008). Figure 5 shows a conceptual illustration of SERS.

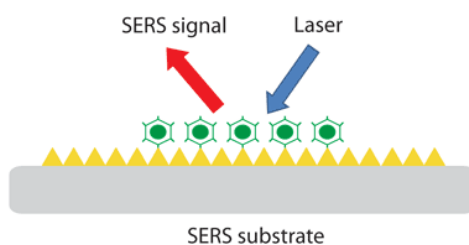


Figure 5: Conceptual Illustration of SERS [Semrock.com, 2018]

The irreproducibility of early enhancement techniques stemming from the varied nature of electrochemical etching hindered the use of SERS as a consistent analytical tool. The advancement of nanofabrication in the late 1990's led to more consistent SERS substrates and thus to a high degree of reliability. The ability to consistently identify an analyte on the level of a single molecule (Emory and Nie, 1997) stimulated growth in the field of SERS. Using metal nanoparticles has become a common method for SERS (Stiles et al., 2008).

C. SERS FOR THC/DRUG DETECTION

SERS for drug detection has become a topic of interest among researchers due to the potential for point-of-care detection. By combining microfluidics with a portable Raman spectrometer, researchers have been able to identify trace amounts of methamphetamine and other substances (Quang et al., 2008; Andreou et al., 2013). Successful techniques flow colloidal metal nanoparticles through microfluidic channels with the analyte in order to allow good mixing of the two. The analyte adsorbs to the metal nanoparticles and provides the enhancement for the Raman signal.

Only recently have scientists begun to utilize SERS for the detection of THC. The first such endeavor utilized a capillary platform prepared by the *in situ* microwave synthesis of gold nanoparticles (Yüksel et al., 2016). The microwave synthesis technique allows for quick batch production of gold nanoparticle coated glass capillaries. The simplicity of analyte collection by capillaries could allow for routine analytics. The researchers confirmed THC detection down to 1 nM through this method. The ability to detect to such a low level indicates SERS is a viable means for THC detection. THC has also been detected using SERS when the THC has been extracted from saliva (Inscore et al., 2011). All efforts to detect THC utilizing SERS have relied upon liquid

phase sample analysis; the research presented here utilized a THC-methanol solution, with analysis being performed after methanol evaporation. Future works will attempt gas phase analysis with simulated breath samples.

D. THC DETECTION IN GAS PHASE/EXHALED BREATH

While SERS has not been utilized to detect gaseous THC, other methods have been used. Liquid chromatography-tandem mass spectrometry (LC-MS) and field asymmetric ion mobility spectrometry (FAIM) have found success in identifying THC in exhaled breath. An electronic nose approach has also successfully identified different forms of cannabis-based drugs based from gaseous samples. Several different research groups have utilized LC-MS as a detection method.

Early attempts using LC-MS established exhaled breath as a promising medium for the analysis of THC (Beck et al., 2011). Samples were collected from patients using a mouthpiece and an Empore disk. The disk was then treated with various chemicals in order to prepare it for LC-MS. Beck et al. were able to quantify the amount of THC in exhaled breath for 1 to 2 hours after use. However, the researchers were unable to detect the primary metabolite THC-COOH. Researchers from the National Institute on Drug Abuse and Karolinska University Hospital detected THC in breath by methanol extraction from breath pads, solid-phase extraction, and LC-MS quantification (Himes et al., 2013). The researchers quantified THC detection for 50 pg/pad and determined THC could be detected for between 0.5 to 2 hours after inhalation. The primary metabolite THC-COOH was able to be detected as well, with a lower limit of 100 pg/pad. A third study utilizing LC-MS was able to detect THC in exhaled breath of volunteers and correlate it to physiological changes (Coucke et al., 2016). THC-COOH was unable to be detected. The

researchers were able to detect THC over 3 hours after smoking with a mean concentration of 1479 pg/sample.

The researchers utilizing LC-MS analyzed real breath samples from volunteer participants. Other researchers utilizing FAIMS were able to detect THC in simulated breath samples down to 65 ppb (Mohsen et al., 2014). Breath samples were simulated by taking a stock THC-methanol solution and heating in an oven to evaporate the methanol. A mass flow control then used dry air to dilute the samples to desired concentrations. The electronic nose method collected gaseous samples by having cannabis plants in a chamber and flowing nitrogen to feed the sample to the electronic nose chamber. The researchers were able to successfully calibrate the electronic nose to identify different cannabis buds, plants, or hashish (Haddi et al., 2011).

Of the presented methods to analyze THC in breath, three utilized LC-MS, one utilized FAIMS, and one utilized an electronic nose approach. The FAIMS and electronic nose methods have been presented as a method for real time diagnostic for analyzing gaseous samples; the FAIMS technique is aimed at THC in breath, albeit a simulated breath sample. SERS has been utilized to identify THC in liquid samples but not in simulated breath samples and thus proves to be an opportunity to expand knowledge in the field of THC detection. A summary of recent studies for THC detection is pictured in Table 1.

Table 1 Summary of THC Detection Research

Author	Detection Method	Sample Medium	LOD	LOD (pg)	LOQ	LOQ (pg)
Teixeira et al, 2007	LC-MS	Oral fluid	2 ng/mL	2000	5 ng/mL	5000
Teixeira et al, 2004	LC-MS	Spiked oral fluid	1 ng/mL	1000	2 ng/mL	2000
Beck et al, 2011	LC-MS/MS	Exhaled breath	2.5 pg/filter	2.5		
Himes et al, 2013	LC-MS/MS	Exhaled breath	50 pg/pad	50	50 pg/pad	50
Coucke et al, 2016	LC-MS/MS	Exhaled breath	3 pg/filter	3	6 pg/filter	6
Milman et al, 2010	GC-MS	Spiked oral fluid	0.5 ng/mL	500	0.5 ng/mL	500
Moshen et al, 2014	FAIMS	Simulated breath	65 ppb	65000		
Amjadi et al, 2014	SERS	Methanol soln	0.065 µg/mL	65000		
Yüksel et al, 2016	SERS	Methanol soln	0.25 nM	78.6	1 nM	314.5

E. MICROPILLARS AS SERS SUBSTRATE

Micropillars, nanopillars, and nanowires possess a wide array of functionality in microfabricated devices. Micropillars and nanopillars have been incorporated into micropreconcentrators (Li et al., 2013), microreactors, photovoltaics (Peng et al., 2005), and adhesives (Aksak et al., 2007). More relevant to this thesis, micropillars and nanowires have also been successfully utilized as a mixing aid or a substrate for SERS. As discussed in Section B, surface roughness increases the potential for excited local surface plasmons which in turn help create scattering. An array of nanowires or nanopillars can provide the necessary surface roughness for SERS.

Liu et al. successfully utilized a hexagonal micropillar array functionalized with gold nanoparticles to produce reliable SERS activity (2015). Nanowires modified with silver have successfully been utilized by researchers to create signal enhancement. Fang et al. metalized a silicon nanowire array with silver nitrate, covering the silicon nanowires with silver nanoparticles (2009). The researchers were able to directly use the metalized nanowires for Raman signal collection with an enhancement factor up to $\sim 10^6$. Shao et al. similarly used silver nitrate to modify silicon nanowires and were able to detect 25 μL of 1×10^{-16} M Rhodamine 6G (2008).

There are various methods available to create a micropillar or nanowire substrate for SERS activity. The two main methods of interest for this thesis are dry silicon etching and wet silicon etching.

F. DRY ETCHING

Dry etching consists of selectively etching the surface of a material by physically bombarding the material with ions, chemically etching through a reaction at the surface, or by combining the two mechanisms (Madou, 2011). Popular dry etching techniques include plasma etching, ion-beam etching, and reactive ion etching.

In plasma etching, a feed gas such as fluorine interacts with a plasma and diffuses to the substrate. The feed gas and the plasma form a volatile product in the substrate and causes the etching. Li et al. utilized plasma etching to create a “nanoforest” of silicon to use as a SERS substrate (2017). Figure 6 illustrates the fabrication process. To create the dense nanoforest array, the researchers spin-coated polyimide onto a silicon wafer. Oxygen plasma treating applied to the polyimide created vertical nanofiber bunches. These polyimide nanofibers acted as a mask for

silicon to create nanopillars. Cl_2/HBr gas source plasma etching created the nanoforest. Stripping the polyimide with acid and then depositing a thin metal layer completed the process. Figure 7 shows the morphology of the final product. The final morphology proves advantageous due to the high feature density which allows for signal enhancement.

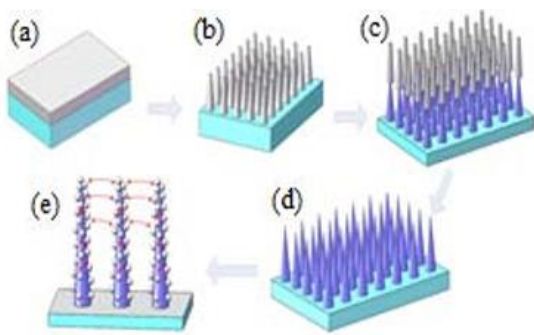


Figure 6- Polyimide Method: a) PI spun on; b) Plasma treating PI; c) Plasma etching; d) Wet etching; e) Metal deposition [Li et al., 2017]

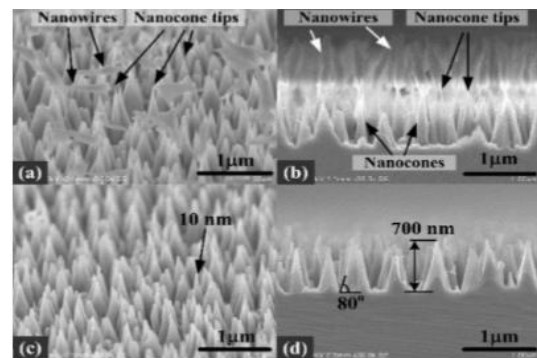


Figure 7- Morphology of Polyimide Method [Li et al., 2017]

Reactive ion etching utilizes high energy, chemically reactive plasma to etch the substrate. Inert ions from the plasma bombard the substrate surface; the momentum transfer from the ions to the surface breaks bonds and causes etching. By combining lithographic or masking techniques with reactive ion etching, micropillar arrays can be fabrication. Deep reactive ion etching (DRIE) is a type of reactive ion etching which cycles between isotropic plasma etching and surface passivation; the alternating steps of etching and passivation allow for vertical, uniform micropillar arrays.

Miller et al. investigated creating vertically aligned micropillars by controlling etch parameters (2012). By altering different etching parameters during the DRIE process, the researchers were able to successfully create a model to predict micropillar profile angle. SF_6 was utilized as for the dry etching while C_4F_8 created the passivation layer. Parameters altered by the researchers include etch time, passivation time, coil power, and platen power. The derived model provides a useful framework for creating vertical pillars and angled features, such as sharp tips on a micropillar. Figure 8 shows the micropillar angle resulting from different process parameters. Figure 9 is the morphology of the micropillars.

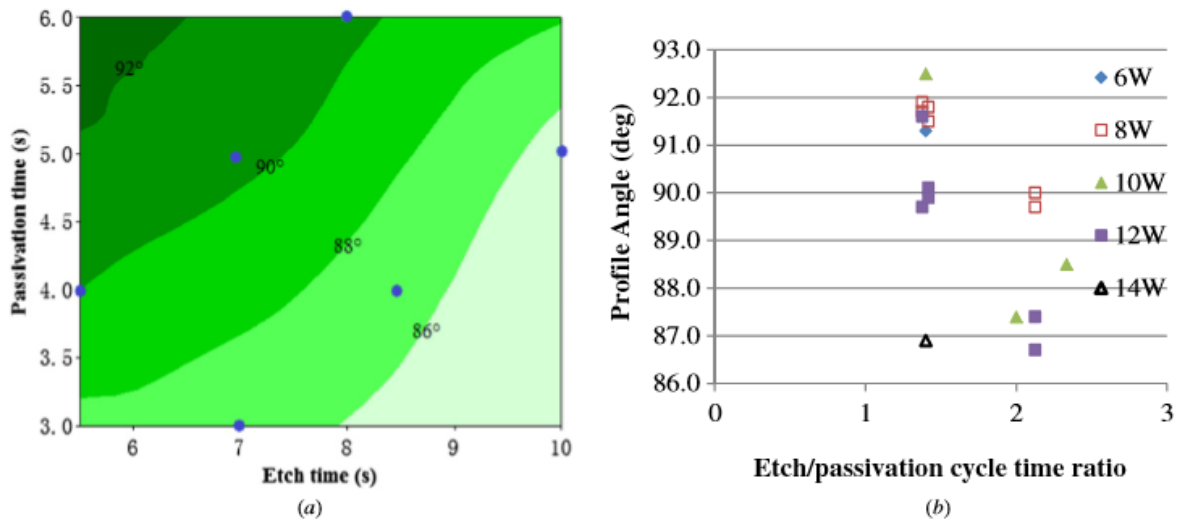


Figure 8- a) Variation of profile angle with etching and passivation times at 600 W and 12 W platen power. b) Profile angle at different etch to passivation cycle times with varying platen power at 600 W coil power. [Miller et al., 2012]

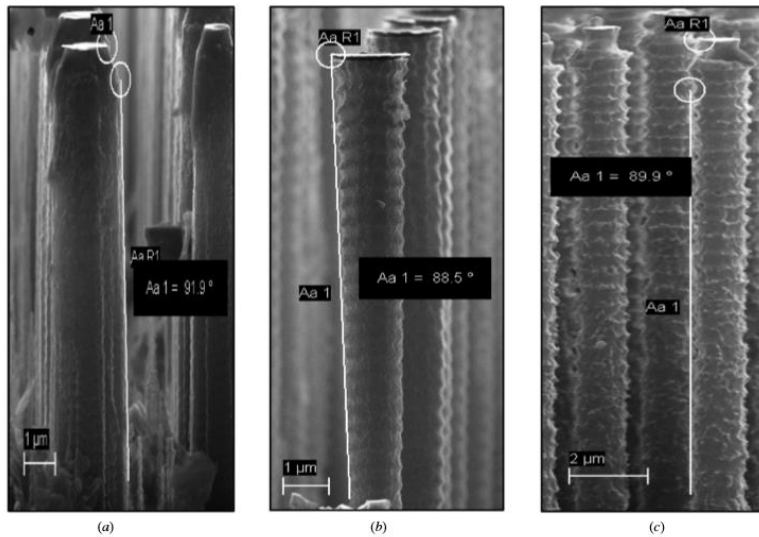


Figure 9- Silicon micropillars fabricated by DRIE exhibiting a) positive ($>90^\circ$), b) negative ($<90^\circ$) and c) near 90° profiles. [Miller et al., 2012]

Liu et al. utilized dry etching to create silicon micropillars functionalized with silver nanoparticles as a SERS substrate (2015). The researchers used photolithography to pattern photoresist on a silicon wafer and then performed deep silicon etching to create the pillars. Germanium nanotapers were grown by chemical vapor deposition and then the pillars were immersed in silver nitrate. The silver nitrate and germanium perform a redox reaction and create silver nanoparticles on the micropillars. Figure 10 details the fabrication process. The researchers achieved an enhancement factor of 1.65×10^7 .



Figure 10- Schematic for the synthesis of Ag-NP@Ge-nanotapers/Si-micropillar hierarchical arrays. [Liu et al., 2015]

G. WET ETCHING

Wet chemical etching techniques can create micropillar and nanowire structures as well. Peng et al. created a process for the fabrication of silicon nanowire arrays for photovoltaic applications (2005). The silicon nanowire arrays were fabricated by treating the silicon wafer with an HF-based aqueous solution containing silver nitrate in a sealed vessel. This process is based on galvanic displacement. The HF/ AgNO_3 solution is thought to create a micro-electrochemical redox process at the silicon surface (Peng et al., 2002). The anodic and cathodic reactions occur concurrently where the metallic atoms being deposited act as a cathode and the surrounding areas as the anode. The HF then selectively etches to create the nanowire structures. Figure 11 shows the chemical etching mechanism and Figure 12 shows the morphology of the nanowires.

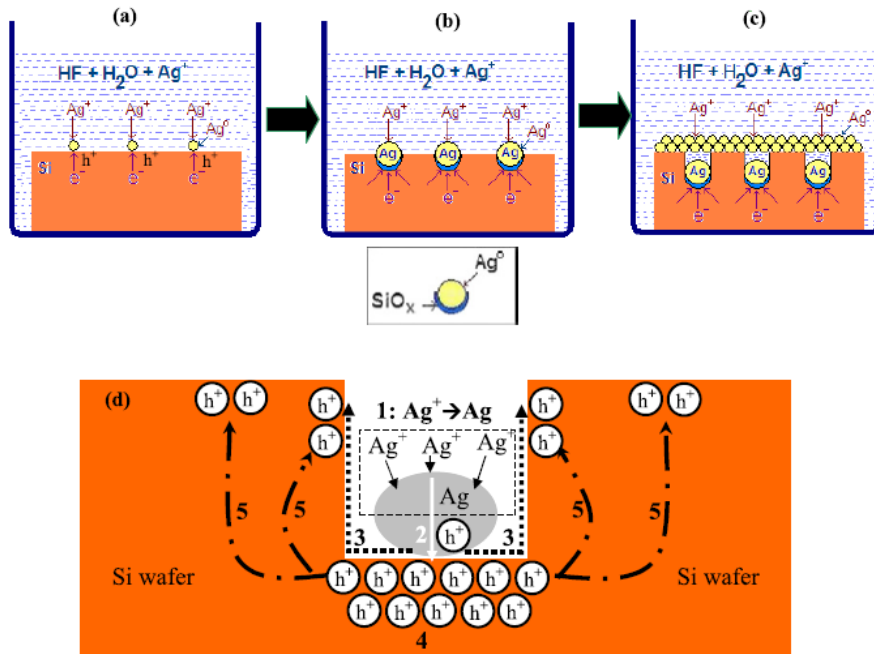


Figure 11: HF/AGNO₃ Etchant Mechanism (Srivastava et al, 2014)

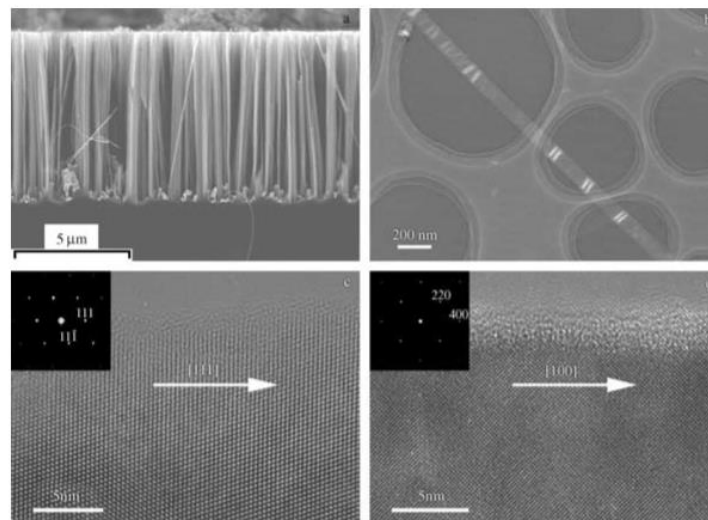


Figure 12- a) SEM cross-section image of silicon nanowire arrays. b) TEM image of an individual SiNW prepared from a p-type (111)-oriented silicon substrate. c) HRTEM image of the nanowire in Figure 1b (the inset is the ED pattern recorded along the [110] axis). d) HRTEM image of a nanowire synthesized from a p-type (100)-oriented silicon substrate (the inset is its ED pattern recorded along the [001] axis). (Peng et al., 2005)

The technique of etching silicon with an HF/AgNO₃ solution has flexibility in the ability to create different morphologies. Temperature, etching time, and solution concentration all influence the final structure of the nanowires (Peng et al., 2002). To create the nanowires pictured in Figure 9, 2.99 g of AgNO₃ was mixed with 50 mL of 50% HF and 200 mL of DI water. The solution was then heated in an open Teflon dish at 50 °C for 2 hours.

H. DRY ETCHING VERSUS WET ETCHING

While both dry etching and wet etching are both able to create microfabricated substrates for SERS activity, wet etching was the more advantageous technique in the case of this thesis. While wet etching necessitates the handling of hazardous chemicals, it eliminates the need for expensive dry etching equipment. The wet etching process to create a nanowire array requires fewer steps and less rigorous processing conditions than dry etching. Wet etching also gives more flexibility in the size of the silicon wafer being etched, allowing for less material to be used to investigate different processing conditions.

III. EXPERIMENTAL

A. EXPERIMENTAL PLAN

Initially the experimental plan was to utilize photolithography, DRIE to achieve micro/nano pillars, and silver sputtering to create a SERS substrate. Research by Miller et al (2012) and Liu et al (2015) provided inspiration for the photolithography and DRIE method. Photolithography was successfully performed; however, DRIE was unable to be attempted due prolonged equipment malfunction. An alternative method consisting of a buffered oxide etch (BOE) and a KOH bath was pursued for a short time. The poor resolution of pillars resulting from this method led to it being taken out of consideration.

Considering the resources available, it was determined that wet chemical etching could provide the desired morphology for the nanopillar substrate. Initial trials were performed following the procedure of silicon nanowire solar cells, as the morphology of the nanowire solar cells could provide a viable SERS substrate (Yang et al., 2008). This method utilized silver nitrate and a hydrofluoric acid solution to etch silicon nanowires. Following removal of the residual silver and cleaning, SEM images revealed the morphology.

The SEM images showed an irregular surface morphology with a multitude of defects, indicating the need for further process optimization. Srivastava et al. (2014) provided clear parameters for achieving different surface morphology of nanowires. The method utilized the same silver nitrate/hydrofluoric acid wet etch of silicon as Yang et al but with different etch parameters. The etch parameters chosen for the presented work were based on the results of Srivastava et al. Micropillars with varying distances between wire bundles were fabricated and tested to determine the optimal SERS substrate. The different surface morphologies were achieved by altering the

silver nitrate and hydrofluoric acid concentrations. Substrates were tested with residual silver from the acid etch and with silver deposited on the surface by sputtering. A qualitative test using a THC-methanol solution as the analyte was performed to determine the viability of the etched, sputtered silicon as a SERS substrate. A quantitative limit of detection test (LOD) test followed to investigate if different THC concentrations yield unique SERS response intensity and to determine the lowest detectable concentration.

B. MATERIALS

1. Silicon Wafer

It was a single-side polished wafer with the following characteristics: Type: N; Grade: prime; Dopant: P; Resistivity: $1-10 \Omega \cdot \text{cm}$; Orientation: $\langle 100 \rangle \pm 0.5^\circ$; Grow Method: Cz; Diameter: $100 \pm 0.2 \text{ mm}$; Thickness: $500 \pm 15 \mu\text{m}$. The wafer was diced into $1 \times 1 \text{ cm}^2$ pieces for processing.

2. N-Methylpyrrolidinone (NMP) Bath

Supplied by Fisher Scientific at 99% purity and diluted. NMP was utilized in cleaning the silicon before etching.

3. Buffered Oxide Etch (BOE)

Supplied by Avantor Performance Materials, BOE is a mixture of ammonium fluoride (30-40%), hydrofluoric acid (1-10%), and water (55-65%). A short BOE bath was the final step of cleaning silicon.

4. Hydrofluoric Acid (HF)

Supplied by Avantor Performance Materials at 49% HF. HF was used to etch silicon and was diluted to various concentrations ranging from 2 M to 12.2 M.

5. Silver Nitrate (AgNO_3)

Supplied by Sigma-Aldrich, 100% purity. Silver nitrate is used in the chemical etch to facilitate creation of nanowires.

6. (-)-trans- Δ^9 -THC Solution

Supplied by Sigma-Aldrich. 1.0 mg/mL in methanol solution. Used as the analyte for Raman spectroscopy. Diluted to various concentrations in high purity methanol.

7. Nitric Acid

Supplied by Avantor Performance Materials, 70% nitric acid solution. Diluted nitric acid was utilized to remove residual silver from silicon after etching.

C. EQUIPMENT

A chemical bench containing an NMP bath was utilized in the cleaning of the silicon wafer. An acid wet bench was utilized as the work station for the HF/AgNO_3 etching of silicon. The acid wet bench had a BOE bath which was used as a cleaning step for silicon and also had a hotplate. The hot plate was necessary to keep the etching solution at 25 °C. All labware coming into contact with HF was required to be Nalgene since HF is corrosive to glass.



Figure 13: Acid Wet Bench



Figure 14: Lesker PVD 75 Sputterer

A Lesker PVD 75 sputterer was used to deposit silver particles onto the silicon nanowires. The sputterer deposited silver by bombarding a disc of silver with energy to release silver particles; the silver particles then deposited on the silicon surface. A relatively low power setting of 150 W was used to deposit the particles. Other specific parameters for the sputtering of silver follow in the procedures. A Dektak Profilometer was used to measure the thickness of the silver deposited

on the silicon nanowire surface. The height difference recorded by the tip of the profilometer arm corresponded to the silver thickness.



Figure 15: Scanning Electron Microscope

The SEM was utilized to image the surface morphology of the silicon post-etching. The images provided details on the nanowire density and silver distribution. The Raman spectrometer was used to identify analyte on the surface of the silicon substrate. A red laser (632 nm) was used to characterize the samples. Software called “Wire 3.4” was used to operate the Raman spectrometer and to record and display the results.

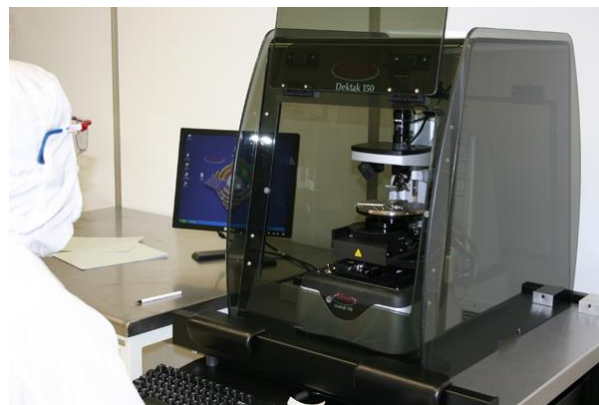


Figure 16: Dektak Profilometer

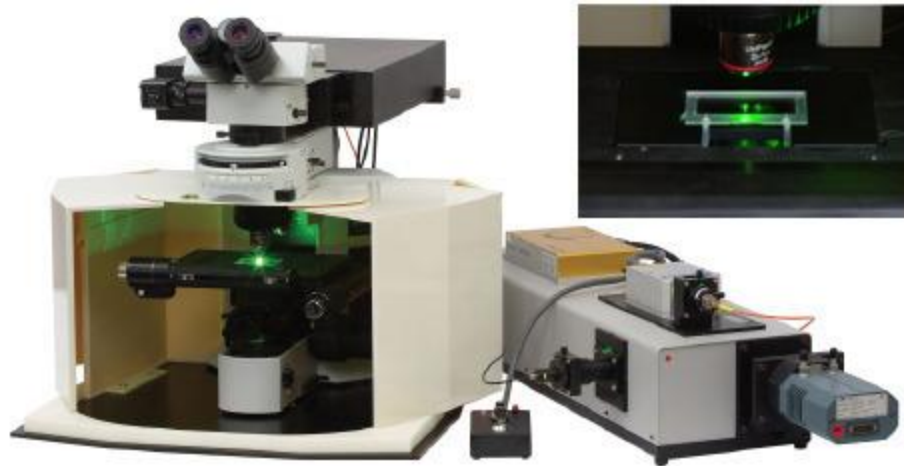


Figure 17: Raman Spectrometer

D. EXPERIMENTAL PROCEDURES

i. Photolithography

1. Obtain a 4 in, 0.5 mm thick single sided Si wafer with a 500 micron thick SiO_2 layer. The wafer was ensured to be clean by washing in the Quick Dump Washer and dried in the Spin Rinse Dryer.
2. Shipley 1805 positive photoresist was spun onto the wafer using a spin recipe of 500 RPM for 1 second and then 4000 RPM for 30 seconds. The wafer was then hot baked on a hot plate at 115 °C for 2 minutes. The spin-coated wafer was then removed from the hot plate and allowed to cool.
3. The next step was exposing the photoresist with UV light. The photomask was inserted into the SUSS mask aligner and ensured to be centered over the wafer. 7

seconds was determined to be the optimal exposure time. The exposure utilized hard contact with the wafer and a light intensity of 12 mW/cm^2 .

4. After exposure a shallow glass container with a developer was used to develop the photoresist. The optimal exposure time was determined to be roughly 15 seconds but may vary based on the age or amount of use the developer has already underwent.
5. After development the quality of the photolithography was assessed by observation under a microscope. The purpose of this step was to ensure the photoresist is not over or under exposed or over or under developed.
6. A BOE bath was then utilized, then a KOH bath. It was then determined that this method did not produce desirable results. An alternative fabrication method using single step wet etching was then pursued.

ii. WET ETCHING SILICON WITH HF/AgNO_3 SOLUTION

a. BY YANG et al. (2008) PROCEDURES

The first attempt at wet etching followed the procedures detailed by Yang et al (Yang et al., 2008). A scale was used to measure out 2.99 g of AgNO_3 . At an acid wet bench, Nalgene labware was gathered in preparation for mixing the etching solution. Proper personal protective equipment (PPE) was donned; this includes chemical resistant gloves, apron, and a full-face shield.

DI water was poured into a beaker and then precisely 200 mL was measured using a graduated cylinder. The water was poured in a 1000 mL Nalgene beaker which served as the container for etching.

Next, roughly 50 mL of 49% HF was poured into a separate Nalgene beaker. A Nalgene graduated cylinder was then used to precisely measure 50 mL of HF. The 50 mL of HF was then slowly poured into the etching beaker.

Next the AgNO_3 was poured into the beaker. A stirring stone was put into the beaker and the beaker was set on a hot plate. The solution was mixed at 200 RPM until the AgNO_3 dissolved. The stirring stone was removed, and the solution was heated to 50 °C.

Once heated, a 1 cm X 1 cm piece of silicon wafer was lowered into the solution with a Nalgene basket for etching. The solution was etched for 2 hours.

After etching the basket containing the wafer was washed in the quick dump rinse.

After etching the wafer pieces were covered in silver dendrites; the wafers were physically removed from the silver and washed. The silver and the used etching solution was disposed in a hazardous waste container.

b. BY SRIVASTAVA et al. (2014) PROCEDURES

The steps for following the procedures set by Srivastava largely remained the same as previous except for changing etching parameters. A few improvements introduced in the presented work were also made to improve etching results. As before, the same labware setup was utilized. Varying HF and AgNO_3 concentrations were utilized for different trials. Cleaning steps were

added before etching to ensure the silicon chips were free of contaminants. Cleaning consisted of a roughly 2-minute rinsing with acetone followed by a 1-minute NMP bath. Water was then used to rinse off any residual NMP and the silicon chip was dried with nitrogen. Next, a 10 second soak in BOE at the acid wet bench. The last step of the preprocess cleaning was to move the silicon chip from the BOE bath to the quick dump rinse for a water rinse. The etching solution temperature was lowered to 30 °C and the etching time was lowered to 1 hour. A nitric acid bath post-etching was introduced to remove residual silver on the silicon chip. The bath consisted of 40 mL of water and 10 mL of nitric acid. The silicon chip was left to soak in the bath for 10 minutes and agitated periodically. After the bath, the silicon chip was washed in the quick dump rinse.

iii. SPUTTERING OF SILVER

Sputtering was performed with the goal of depositing silver particles on the surface of the micropillars. Different settings were investigated to deposit a thin layer of silver (~25nm). The investigation is detailed in Section IV. The final settings used for the experiments are shown in the Table 2.

Table 2: Optimized Sputtering Conditions

Sputtering Conditions	
Metal	Silver
Power	150 W
Pump Time	60 min
Deposition Time	1 min
Deposition Rate	~25 nm/min

First, the silver deposition rate was determined utilizing a taped-off glass slide as a substrate. A spare 4-inch silicon wafer was necessary to mount the glass slide for sputtering. Three

pieces of tape across the glass slide affixed it to the silicon wafer. Sputtering deposits silver on the surface of the glass slide and the tape. When the tape is removed, the glass slide beneath is exposed. The height difference from the glass slide and the silver layer was then measured with the profilometer (see next section). Once the desired silver thickness was achieved, the etched silicon chip is taped to the glass slide and sputtered.

The first step for sputtering was to vent the Lesker PVD 75 sputterer. The first step was loading the target (silver) into the PVD 75. The door was opened once the chamber was vented. The source shutter for the target was opened and the gas inlet tube was removed. The dark space shroud was removed followed by removing the rings for holding the target in place. The silver was placed at the target and affixed with the rings and shroud. The gas inlet tube was replaced.

Next a digital multi-meter was used to check for continuity. This ensures the silver target and the shroud are electrically isolated. Once continuity was confirmed, the source shutter was closed as was the door to the PVD 75. Next the substrate was loaded. To load the substrate, the substrate shutter was opened from the control screen. The substrate access panel was removed and the silicon wafer with the glass slide taped to it was inserted facing downward (toward the silver source). The access panel was replaced and the substrate shutter was closed. The machine was then vented. Once pumped down for the desired time, the argon gas flow was set to a constant rate and the DC power supply for the silver source was set to the desired power. The source shutter was then opened for the desired deposition time. Once reaching the deposition time, the shutter was closed and the source powered down. The machine was vented and the silver source and the sample were removed from the PVD-75.

iv. PROFILOMETER MEASUREMENT

The Dektak Profilometer was used to measure the thickness of the silver deposition layer. The thickness of the silver deposition could then be divided by the deposition time from silver sputtering to get the deposition rate. The deposition rate was useful to know because it allowed for more efficient optimization of the sputtering settings. A relatively linear relationship between the sputtering source power and deposition rate made for easier optimization.

The profilometer used a precise stylus tip to measure the height difference between surfaces. The height difference was the thickness of the silver layer. To load the sample in the profilometer, the glass slide was left on the silicon wafer. Tape was removed, exposing the surface of the glass slide. Next the guard panel to the profilometer was opened and the load/unload command was entered. The stage of the profilometer moved forward and the silicon wafer with the glass slide on top was placed in the loading area. The stage was returned to the center and the guard panel was closed. Next, the “tower down to null position stylus up” icon was pressed. This lowers the stylus to the substrate surface, then releases it slightly to allow for repositioning. The stylus was positioned to run perpendicular to the groves left from the tape removal. Scan parameters were adjusted. Force applied to the stylus was set to 3 mg, the measurement range was set to 655 kA, and the profile was set to hills and valleys. The scan went from the silver surface, down to the glass substrate, and back to the silver surface again. Once the scan was complete, a level section of the silver dataset can be set to zero. This then shows the step difference when the stylus moves to the valley made by the tape and gives the measurement of the silver thickness.

v. SCANNING ELECTRON MICROSCOPY

Surface morphology of etched silicon was viewed using a scanning electron microscope. Images were taken from a top down view and at a 20° angle. The samples were affixed to the viewing stage in the SEM and the chamber was flushed with nitrogen. Once focused on the surface, different areas of the sample were imaged. Results from the surface morphology informed changes to etching parameters to achieve the desired surface morphology. SEM images can be viewed in Section VI.

vi. RAMAN SPECTROSCOPY

Raman spectroscopy was used to characterize the silicon samples and to see if the etched silicon nanowire structure with silver could provide enough enhancement to detect trace levels of THC. Sample were prepared for Raman spectroscopy by cleaning the silicon chips with methanol. The analyte of THC in methanol solution was pipetted onto the silicon chip and then put in the Raman spectrometer for analysis. See Section IV for more details on the THC-methanol analyte. After sample preparation, the Raman spectrometer is set up. On the attached computer, “Wire 3.4” program was used to run the Raman and record and display the result. The laser used was a 632 nm red laser set to 100% power with 1800 nm diffraction grating. These settings were selected in the program and the proper lenses for the laser and diffraction grating were installed in the spectrometer.

The first step to using the Raman spectrometer was to open the Wire 3.4 program. After ensuring the proper settings were selected and the corresponding lenses and diffraction panel were in place, the laser was turned on by a switch on the machine. A light source for the sample

stage was turned on as well to illuminate the sample for the inboard microscope. After opening the sample changer, a sample was placed on the stage under the microscope and the desired magnification was selected in to see surface morphology. The sample stage was able to be manipulated to analyze a specific spot on the chip. Once the desired spot was selected, the image was brought into focus by adjusting the knobs. The sample chamber was closed and dials on the Raman were manipulated to allow the laser to enter the chamber and hit the sample. Focusing of the laser was oftentimes necessary as the laser had to be focused to the specific spot of analysis. Once the laser was focused on the sample, a spectral acquisition was selected from the program. After running the spectral acquisition, the results are displayed on a graph. The data was then saved to a text file and later graphed in Excel.

At the start of each spectroscopy session, a plain silicon sample was run to ensure the Raman spectrometer was working properly. A sharp peak for silicon at 520 cm^{-1} indicated the spectrometer was operating as desired; if there was no silicon response peak, then the settings needed to be adjusted. The etched silicon nanowire substrates were also measured before being treated with analyte; any peaks other than silicon indicated possible contaminants on the surface.

IV. RESULTS AND DISCUSSION

A. PHOTOLITHOGRAPHY

Initially, photolithography and DRIE were pursued as a method to create a silicon micropillar substrate for SERS. As outlined in Section III A., photoresist was to serve as an etch mask for DRIE to create micropillars. However, the prolonged malfunction of the DRIE equipment led to pursuing KOH as an etching method. After the creation of micropillars, sputtering was planned for silver deposition. Figures 18 through 20 show a microscope image of the circular photoresist structures that were to serve as the mask for DRIE. Various pillar arrangements were designed on the photomask to investigate if pillar diameter, distance, and pattern (square grid versus hexagonal) affected SERS activity.



Figure 18: Photoresist pillars on Si, x5 magnification

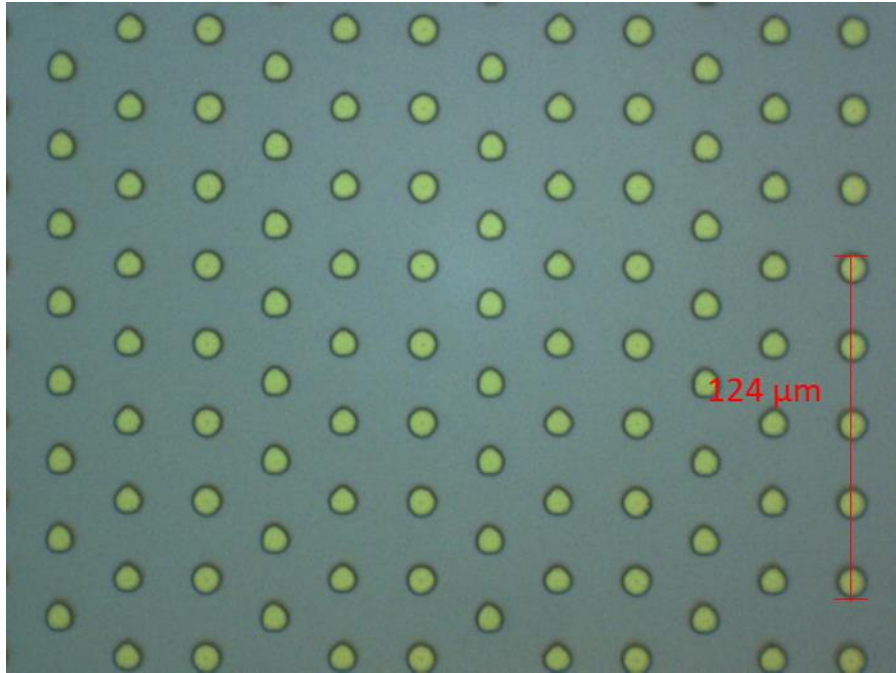


Figure 19: Photoresist pillars, x20 magnification

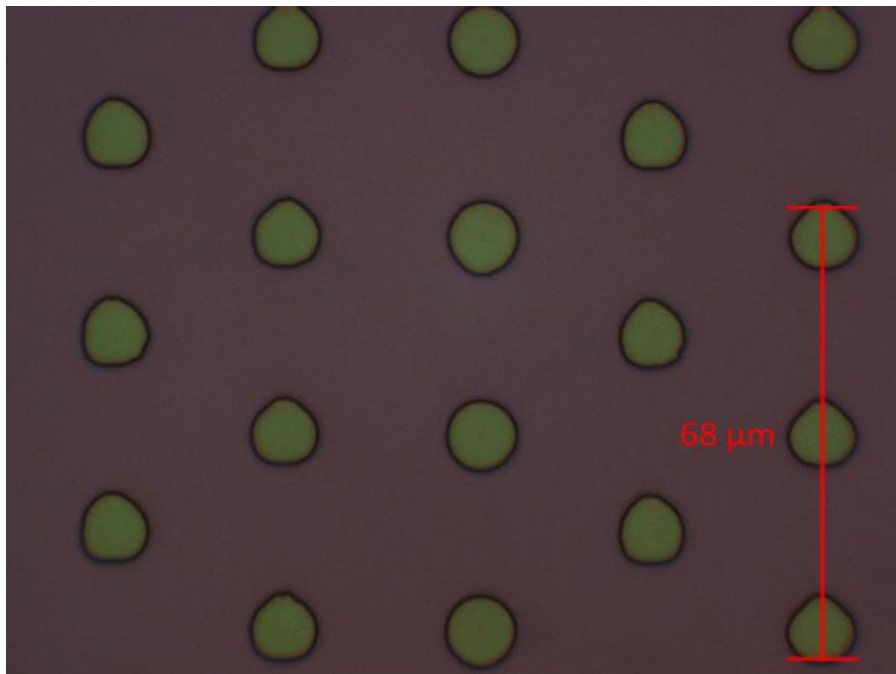


Figure 20: Photoresist pillars, x50 magnification

The full experimental design for photolithography will not be included in the report due to it not being the final method pursued for SERS detection of THC. The decision to pursue acid wet etching with a HF/AgNO₃ stems from three main factors: the prolonged malfunction of the DRIE; the inability to get the photoresist micropillars below 8 microns in diameter without significantly increasing production cost and lowering quality; and the poor initial results from the KOH bath as an alternative to DRIE. Figure 21 through 23 shows the degradation of the surface after the KOH etch.

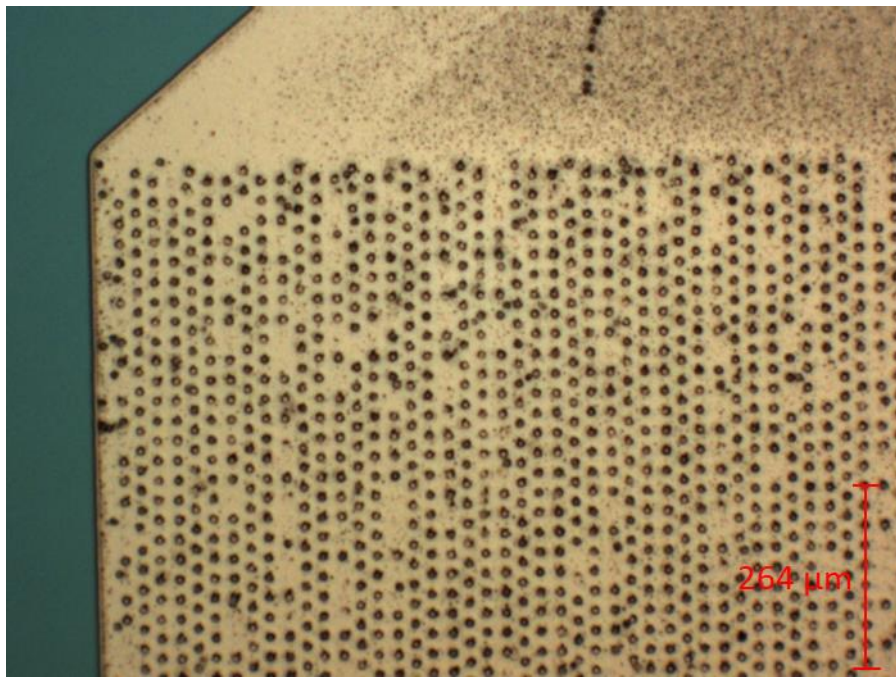


Figure 21: Post-etch photoresist pillars on Si, x5 magnification

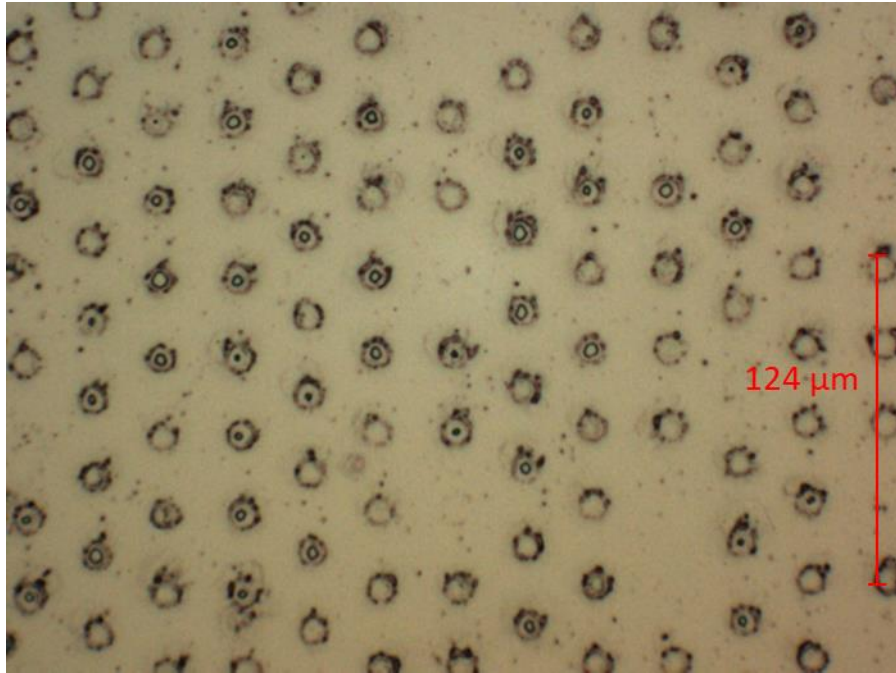


Figure 22: Post-etch photoresist pillars on Si, x20 magnification

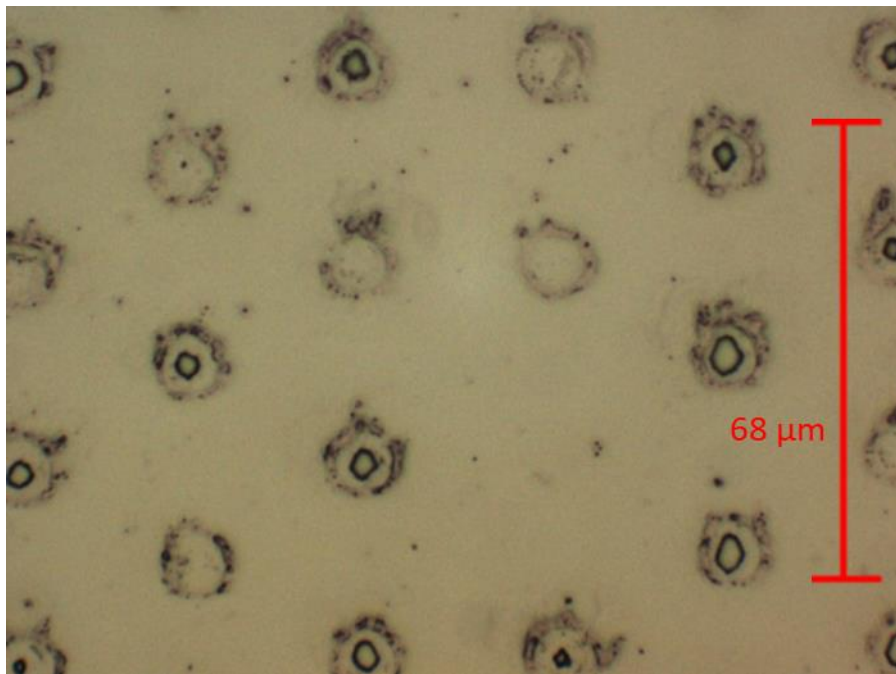


Figure 23: Post-etch photoresist pillars on Si, x50 magnification

While further optimization of the KOH bath may have led to favorable results, wet etching by HF/AgNO₃ had the potential to create a more dense SERS substrate than the photolithography and KOH method.

B. WET ETCHING MORPHOLOGY

a) BY YANG et al. (2008) PROCEDURES

As described in Section III D, an acid wet etch using HF/AgNO₃ to etch silicon was investigated to create a nanowire SERS substrate. Procedures described by Yang et al. (2008) served as the guide for the initial parameters. The etching parameters are detailed in Table 3.

Table 3: Trial 1 and Trial 2 Etch Parameters

	Trial 1	Trial 2
Temperature °C	50	30
HF Concentration (mol/L)	7.14	7.14
AgNO ₃ Concentration (mol/L)	0.07	0.07
Etch Time (min)	120	60

Trial 1 followed the exact procedure outlined by Yang et al. Immediately upon lowering the silicon wafer into the 50°C etching solution, vigorous etching began. The silicon wafer became black in color, bubbles vigorously propagated, and silver dendrites began building on the surface. After the 2 hours etch, the silicon chip was noticeably degraded. The chip was smaller in size and

appeared to have a significant amount of silicon etched away. SEM images reveal the morphology of the wafer as non-uniform. As seen in Figures 23 through 26, it appears silicon nanowires formed but became disarrayed due to the intensity of the etch. The SEM also revealed residual silver on the surface, some in the form of particles and other in the form of dendrites.

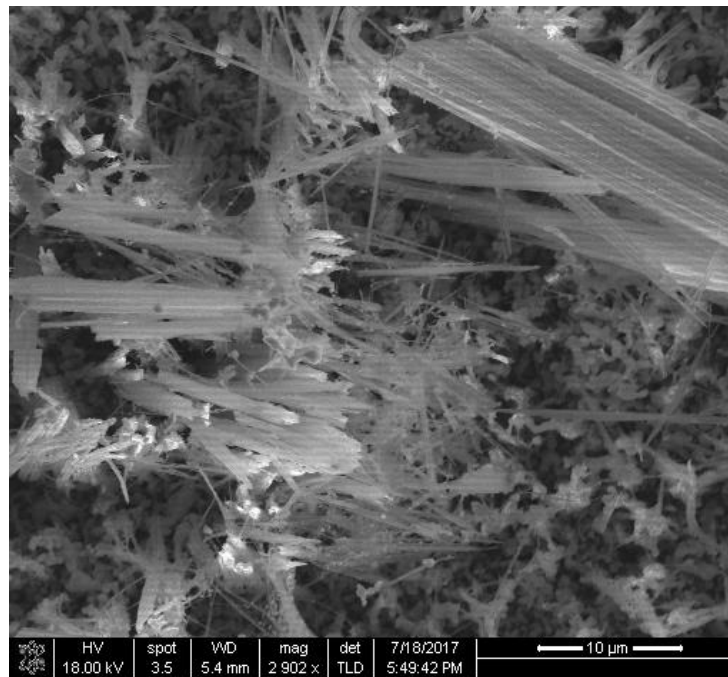


Figure 24: Trial 1, 7.14 M HF, 2 hour, 50°C etch from top down view

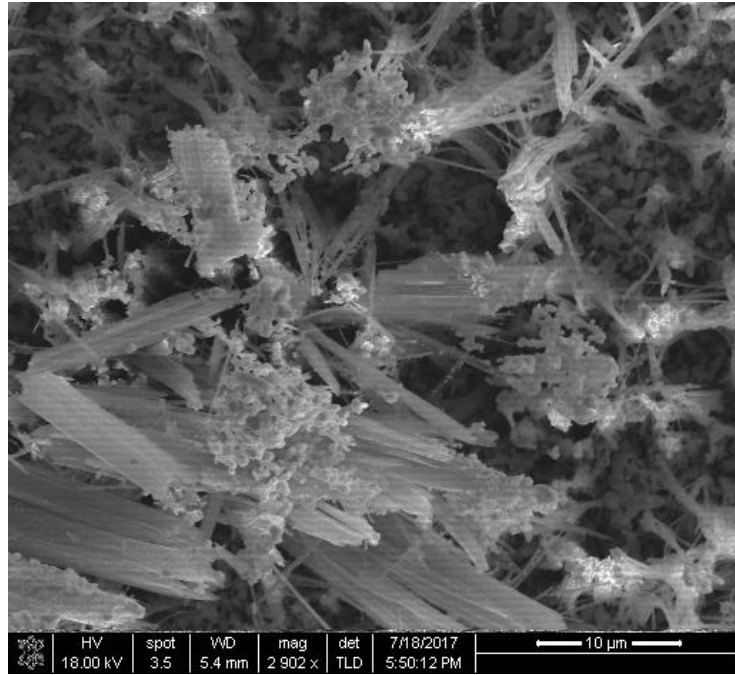


Figure 25: Trial 1, 7.14 M HF, 2 hour, 50°C etch from top down view

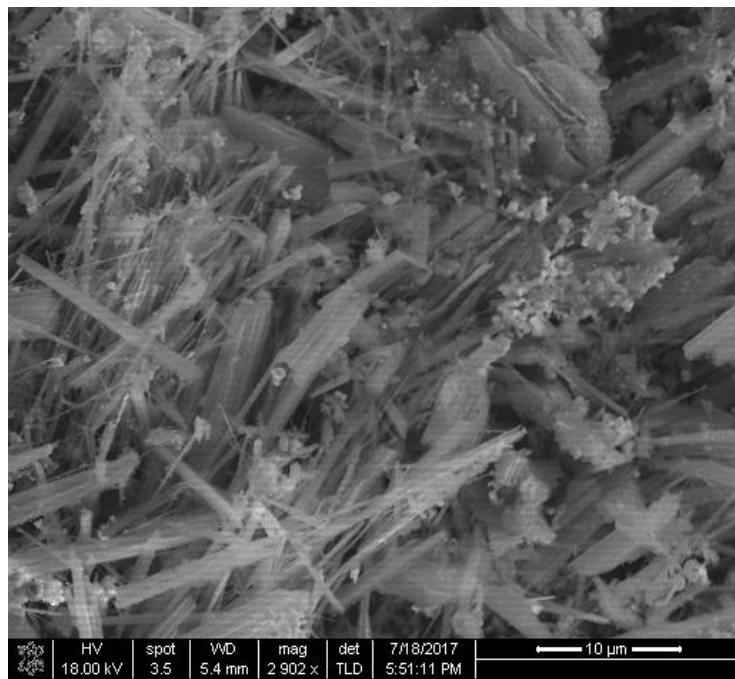


Figure 26: Trial 1, 7.14 M HF, 2 hour, 50°C etch from top down view

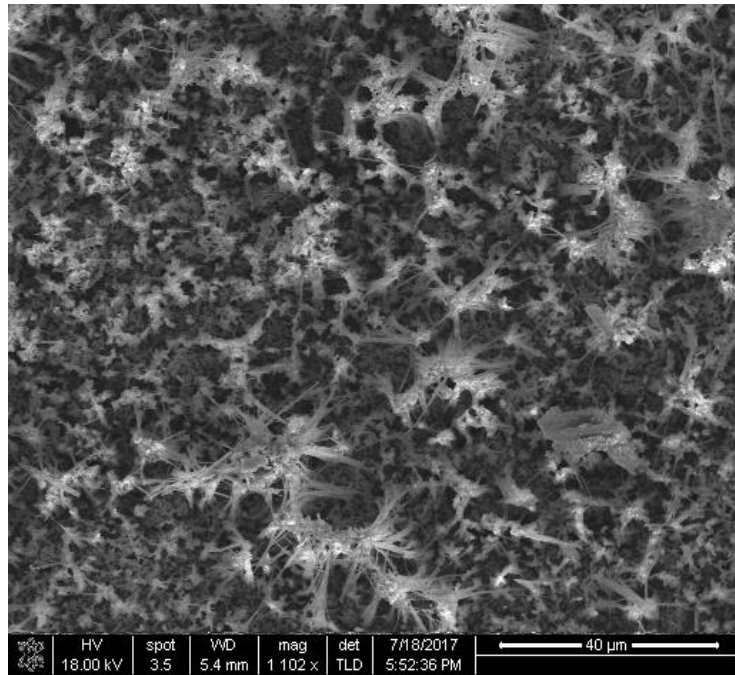


Figure 27: Trial 1, dendritic residual silver from top down view

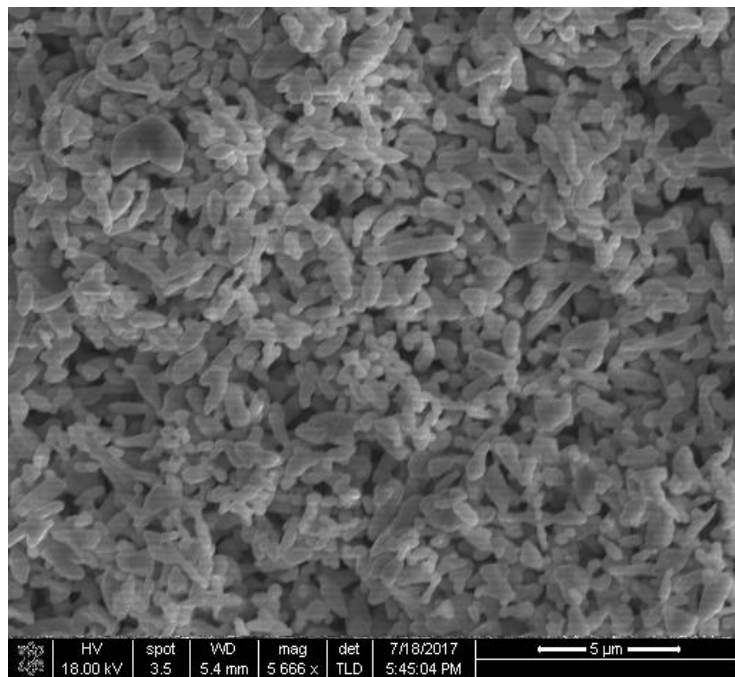


Figure 28: Trial 1, residual silver particles from top down view

Due to the disarrayed surface morphology revealed by SEM images, trial 2 was set to run with a lower solution temperature of 30°C and an etching time of 1 hour. When the silicon chip was lowered into the etching solution, it reacted less vigorously than in trial 1. Instead of immediately blackening, the chip clouded over and slowly blackened. Bubbles formed but not as vigorously and there was less silver dendrite buildup on the surface of the chip. Top down view SEM images revealed a structure similar to the nanowire structure achieved by Yang et al. Deposits of silver still covered significant portions of the silicon surface. These more promising results led to the decision to investigate varying concentrations of HF and AgNO₃ on the surface morphology with the goal of finding which morphology created the best Raman signal enhancement.

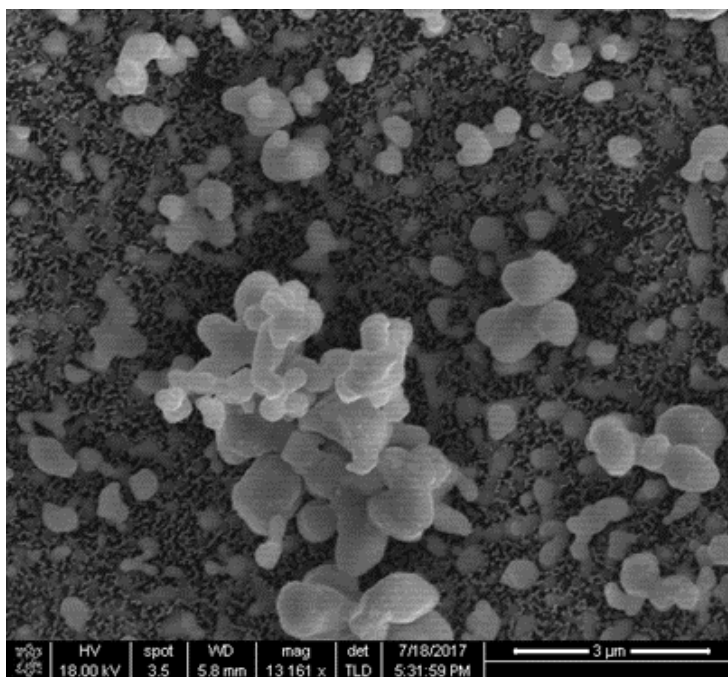


Figure 29: Top view of trial 2, 1 hour, 30°C etch

b) BY SRIVASTAVA et al. (2014) PROCEDURES

While Yang et al. proved a good starting point, Srivastava et al. performed an in-depth investigation into the influence of HF and AgNO₃ concentration on silicon nanowire morphology. The first set of trial parameters by done by this method are listed in Table 4.

Table 4: Trial 4 through 6 Parameters

	Trial 3	Trial 4	Trial 5	Trial 6
Temperature °C	30	30	30	30
HF Concentration (mol/L)	2.00	10.40	5.00	7.90
AgNO ₃ Concentration (mol/L)	0.01	0.01	0.02	0.02
Etch Time (min)	20	20	20	20

Trial 3 and Trial 4 were run first. Upon lowering the silicon chip into the respective etching solutions, reactivity appeared to be low. For Trial 3 there was bubbling and some silver dendrite build up. However, it was to a lower degree than before. For Trial 4 there was minimal bubbling and almost no silver dendrite formation. Silver dendrite formation on the silicon chip during etching was desirable because it indicates successful etching of the silicon. The low formation of silver dendrites prompted an increase of AgNO₃ concentration for Trails 5 and 6. SEM images of Trials 3, 4, 5, and 6 are pictured in Figures 30 through 33.

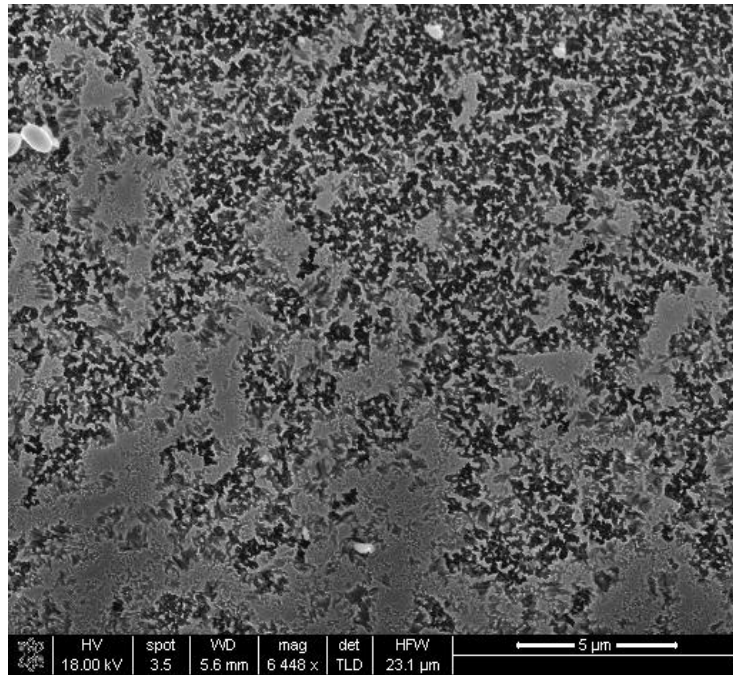


Figure 30: Trial 3, 2.00 M HF viewed from top down

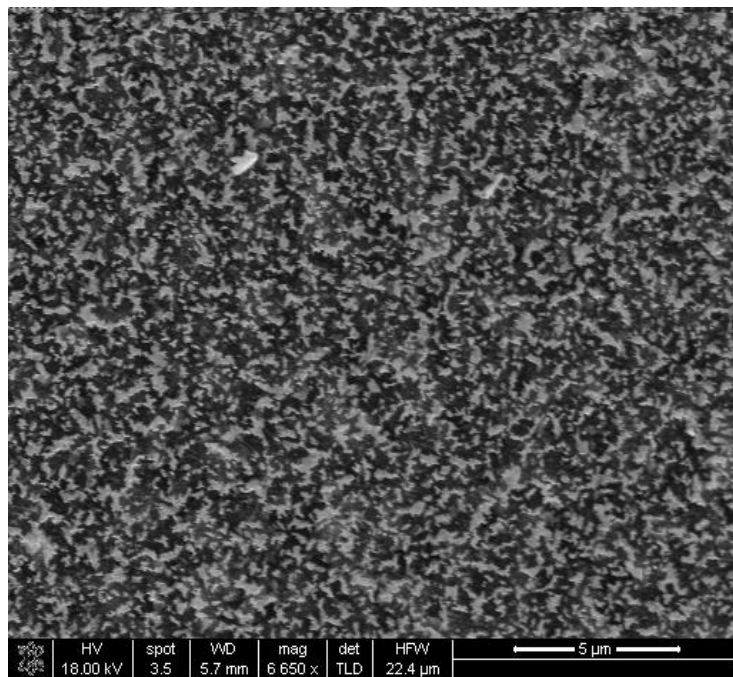


Figure 31: Trial 5, 5.00 M HF viewed from top down

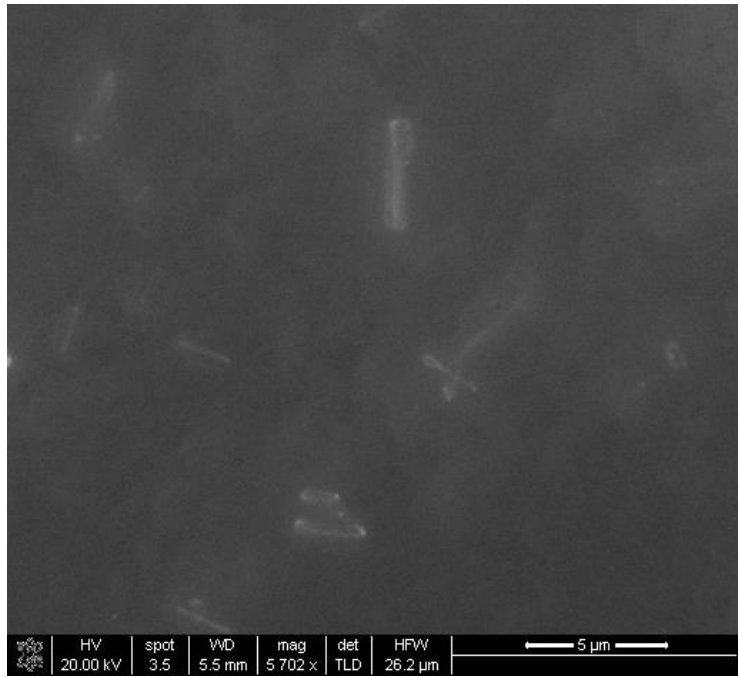


Figure 32: Trial 6, 7.90 M HF viewed from top down

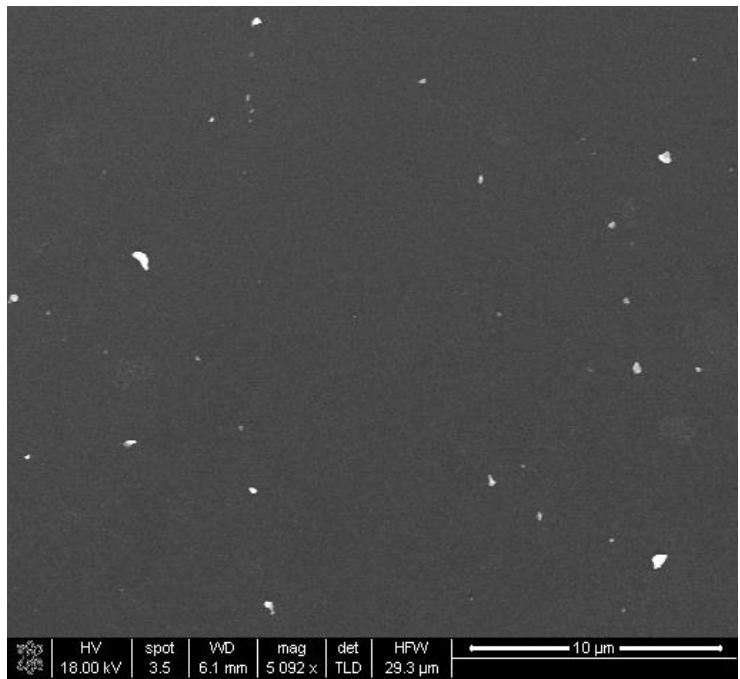


Figure 33: Trial 4, 10.40 M HF viewed from top down

The results from Trials 3, 4, 5, and 6 would indicate the higher HF concentration inhibits etching. However, references suggest Trials 4 and 6 should have etched, so it is likely there was some procedural error in the experiment. It was theorized that the etching time was not long enough, as Trial 3 shows partial etching. This could also be an explanation as to why no nanowire features appear on Trial 4 and Trial 6.

It was decided for the next set of trials to follow Srivastava et al. more closely to replicate their results. The next set of trial parameters are shown in Table 5.

Table 5: Trial 7 through 9 Parameters

	Trial 7	Trial 8	Trial 9
Temperature °C	30	30	30
HF Concentration (mol/L)	2.00	8.15	12.20
AgNO ₃ Concentration (mol/L)	0.02	0.02	0.02
Etch Time (min)	60	60	60

For Trials 7, 8, and 9, all factors were kept the same while HF concentration was varied. Before etching, the cleaning steps outlined in Section D ii. b) were introduced to ensure removal of surface contaminants before the etch. Also introduced was the post-etch nitric acid bath to removed residual silver from the silicon surface. Removal of residual silver allowed for better viewing of surface morphology.

Trial 7 began to react immediately once the silicon was lowered into the etching solution. After 30 minutes the chip was covered in a modest amount of silver dendrites and was bubbling slowly. The bubbling was constant but not vigorous. For Trial 8, the etching also visibly began. Etching appeared to be more vigorous than Trial 7 and more silver dendrites built up on the chip. After 30 minutes the chip was covered in silver dendrites and the bubbling was steady. Trial 9 behaved similarly to Trial 7, although to a slightly lesser degree. Trial 9 was more vigorous than Trial 7 but less so than Trial 8.

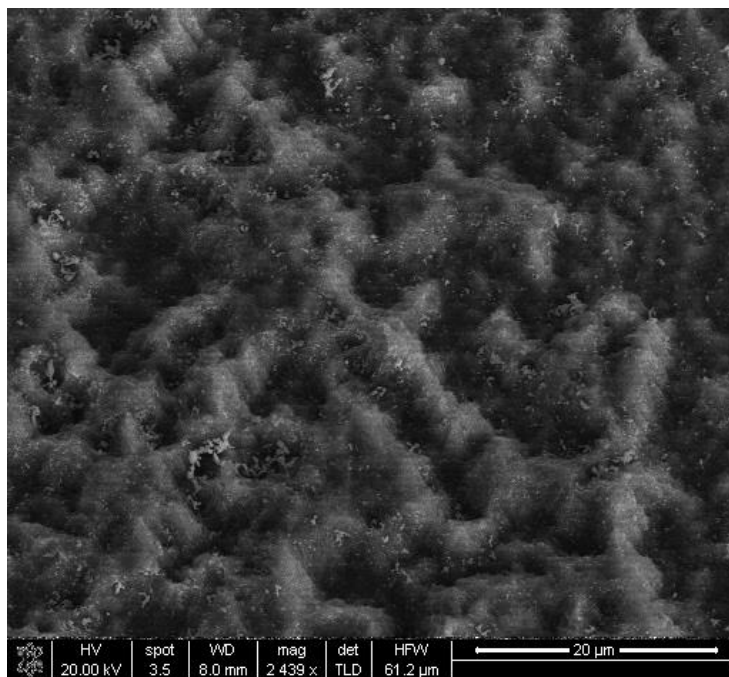


Figure 34: Trial 7, 2 M HF viewed from 20° tilt

The Trial 7 SEM image shows the beginning of nanowire formation. However, nowhere on the chip did the nanowires successfully form. Trial 8 SEM images show large area, uniform nanowire formation.

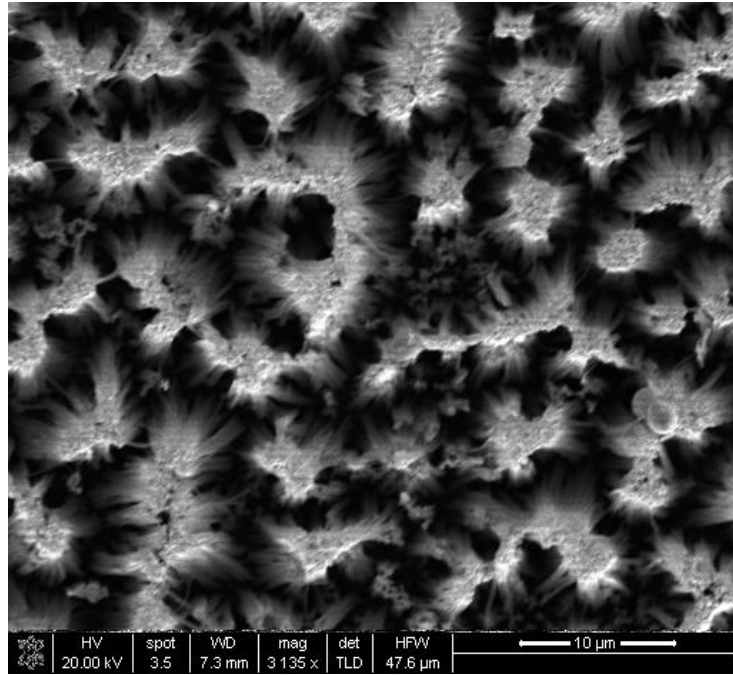


Figure 35: Trial 8, 8.15 M HF viewed from top down

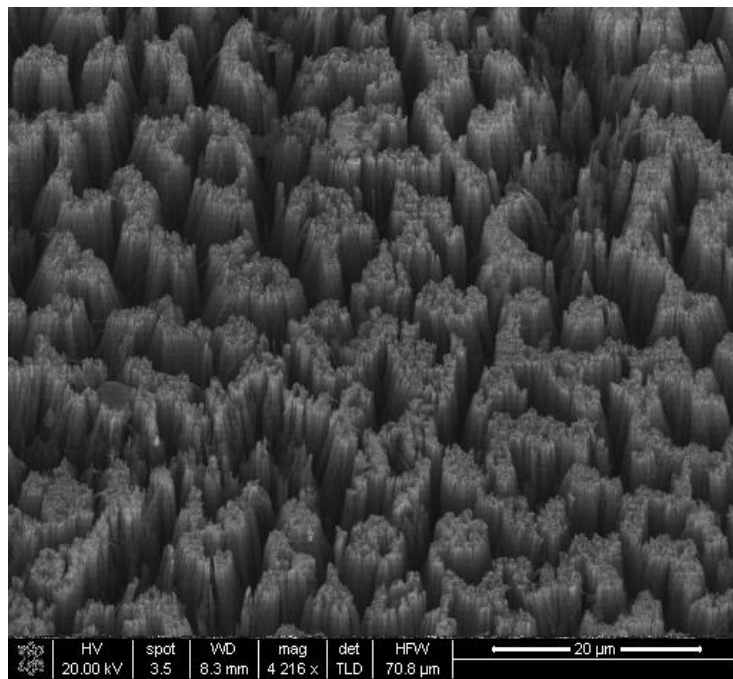


Figure 36: Trial 8, 8.15 M HF viewed from 20° tilt

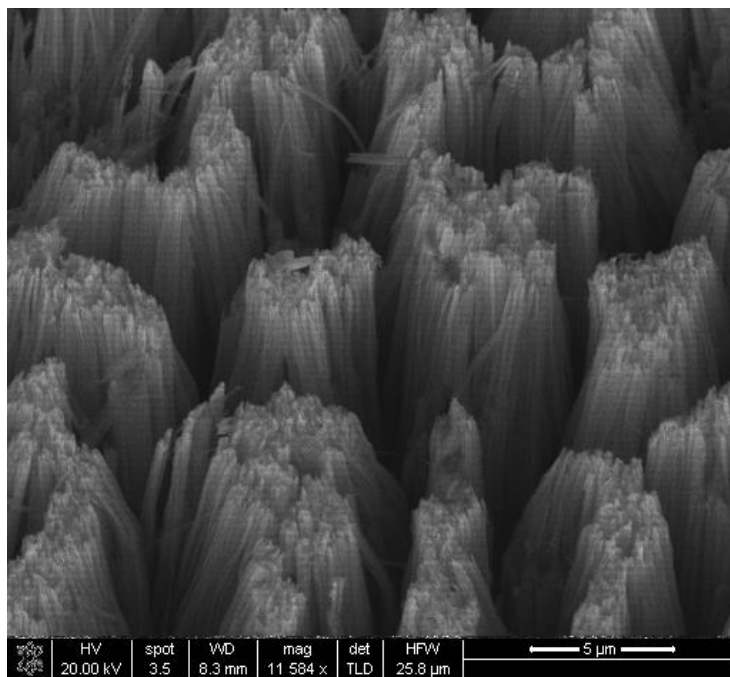


Figure 37: Trial 8, 8.15 M HF viewed from 20° tilt

Trial 9 also shows successful formation of nanowire structures. The successful formation of nanowires at 8.15 M and 12.2 M HF and the unsuccessful formation at 2 M HF led to the decision to add a 5 M HF set of trials for comparison. Also added to investigate was an increase in AgNO_3 concentration to see how it would affect surface morphology and SERS activity.

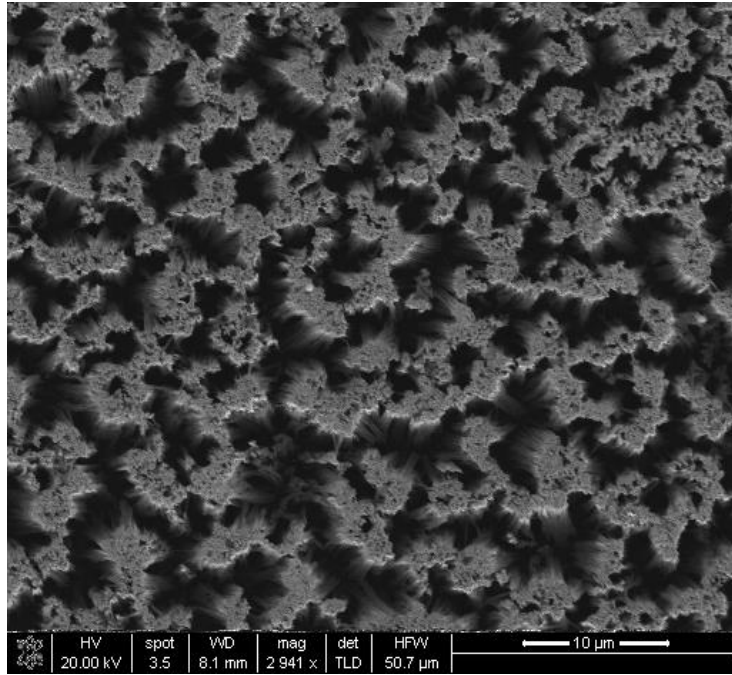


Figure 38: Trial 9, 12.2 M HF viewed from top down

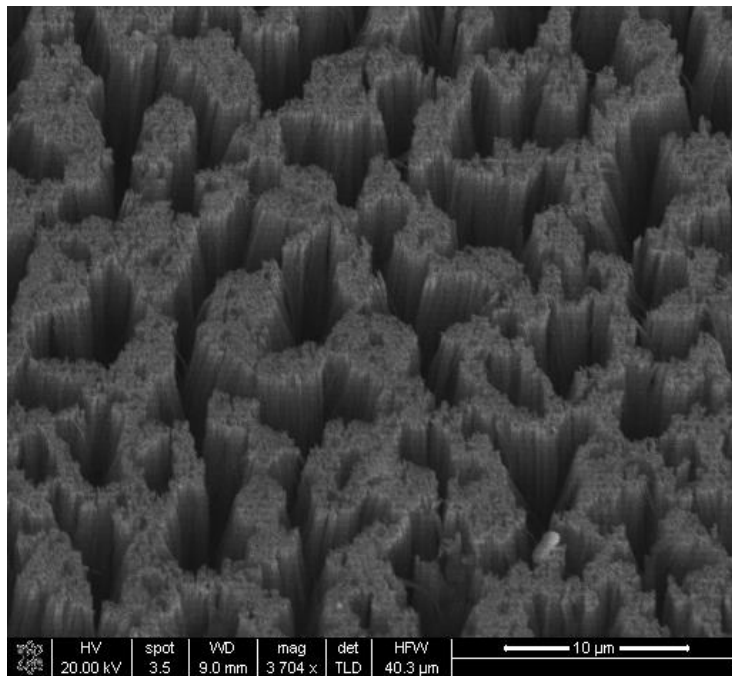


Figure 39: Trial 9, 12.2 M HF viewed from 20° tilt

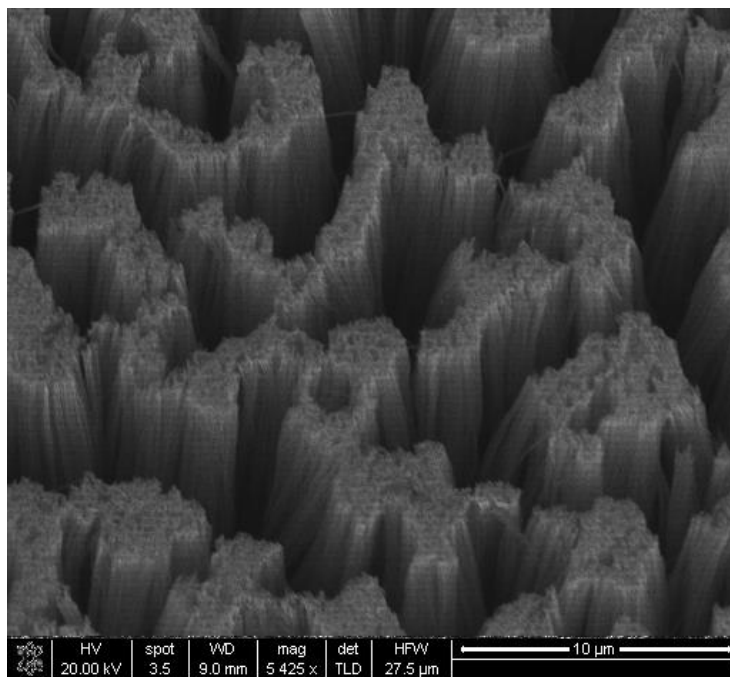


Figure 40: Trial 9, 12.2 M HF viewed from 20° tilt

With the confirmation of nanowire formation from the second set of trials, the third set of trials was performed. The conditions of Trial 8 and Trial 9 were repeated for Trial 12 and Trial 13, respectively. The difference was omitting the nitric acid bath to remove residual silver from the surface of the chip. For Trials 10 through 11, surface silver was not removed so as to later investigate the SERS performance of residual silver versus sputtered silver. The parameters are outlined in Table 6.

Table 6: Trial 10 through 13 Parameters

	Trial 10	Trial 11	Trial 12	Trial 13
Temperature °C	30	30	30	30
HF Concentration (mol/L)	5.00	5.00	8.15	12.20
AgNO ₃ Concentration (mol/L)	0.10	0.02	0.02	0.02
Etch Time (min)	60	60	60	60

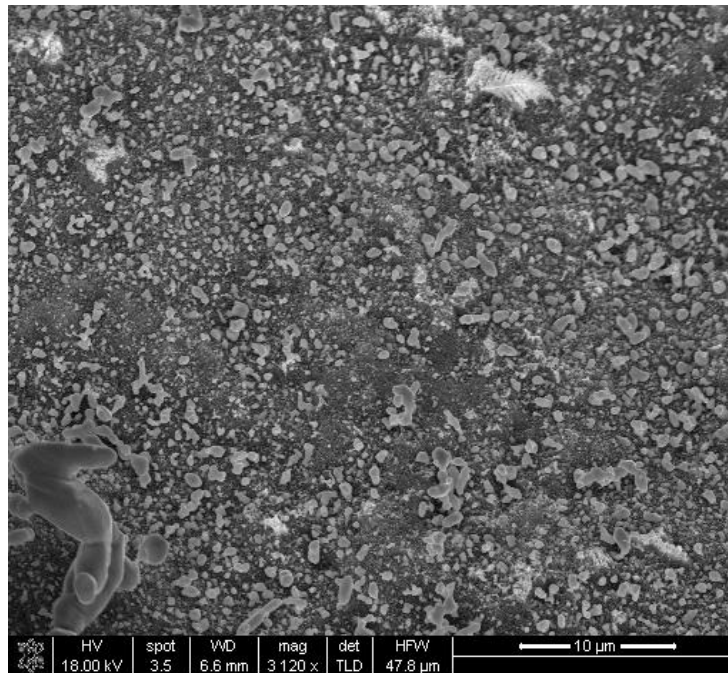


Figure 41: Trial 10, 5 M HF, 0.10 M AgNO₃, top down view

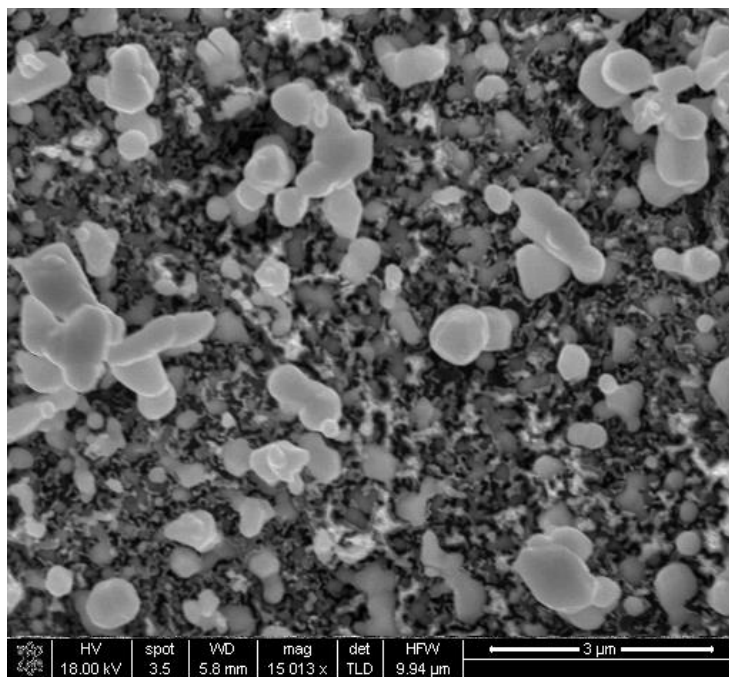


Figure 42: Trial 10, 5 M HF, 0.10 M AgNO₃, top down view

Figure 41 and 42 show images of from the Trial 10 which was run with a higher AgNO₃ concentration of 0.10 M. Trial 10 reacted the most vigorously; the silicon chip immediately was blackened and a steady stream of bubbles began. A large of silver dendrites formed. SEM images revealed the entirety of the silicon surface was covered in a layer silver. Without removing the silver, there was no way to confirm the presence of nanowires. Trial 11 was performed with the same HF concentration as Trial 10, 5M, and with a lower AgNO₃ concentration of 0.02 M. Trial 11 was observed to have similar behavior to Trial 8; steady bubbling and moderate silver buildup on the silicon chip. Under the SEM, micropillars visibly formed and the SEM images show residual silver on the surface as well. Figure 43 and Figure 44 show the Trial 11 silicon surface.

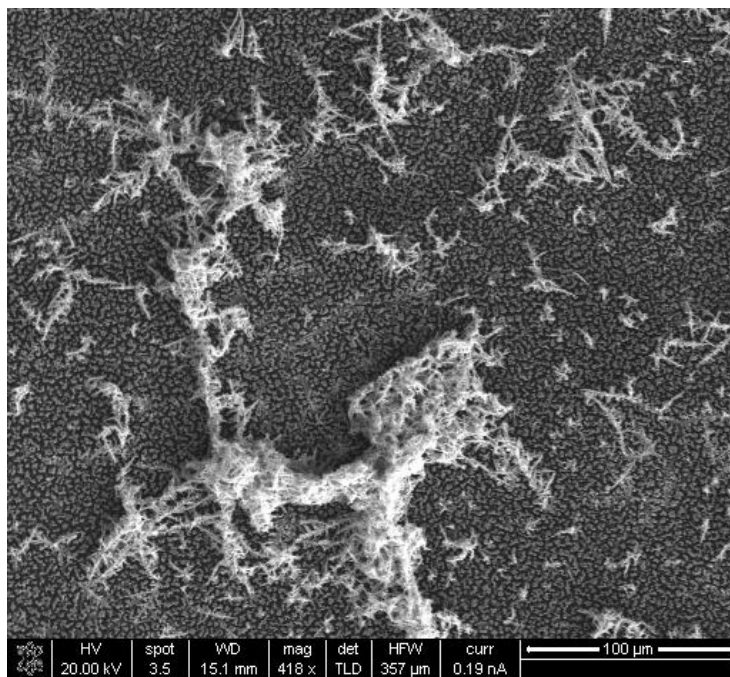


Figure 43: Trial 11, 5 M HF, 0.02 M AgNO₃, residual silver top down view

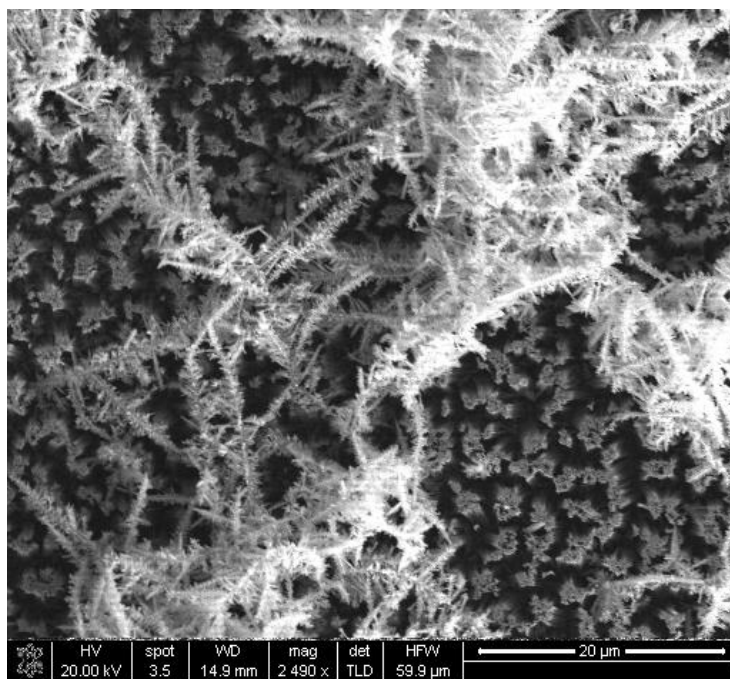


Figure 44: Trial 11, 5 M HF, 0.02 M AgNO₃, residual silver top down view

Figure 43 and Figure 44 show the irregularity of the residual silver. The silver was not spread uniformly across the surface and formed dendritic structures. Figure 45 shows the dendrites in slightly more detail. Figure 46 and Figure 47 show the residual silver resides atop the nanowire structures.

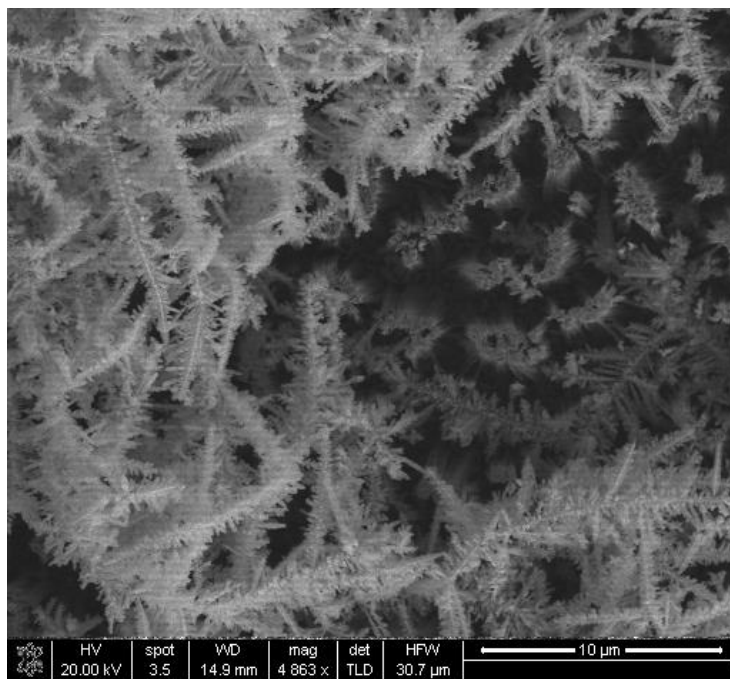


Figure 45: Trial 11, 5 M HF, 0.02 M AgNO₃, residual silver top down view

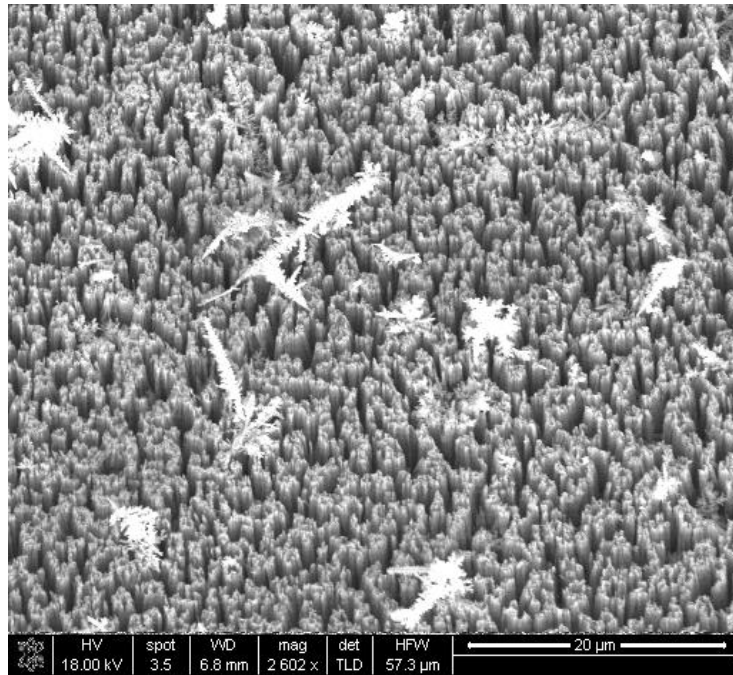


Figure 46: Trial 11, 5 M HF, 0.02 M AgNO₃, residual silver, 20° tilt view

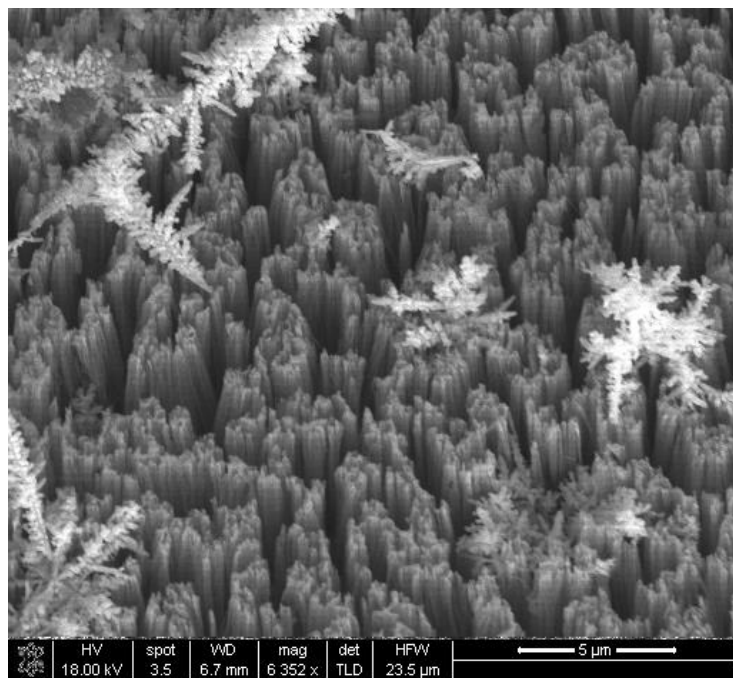


Figure 47: Trial 11, 5 M HF, 0.02 M AgNO₃, residual silver, 20° tilt view

As mentioned previously, Trial 12 and Trial 13 are repeats Trial 8 and Trial 9, respectively, but with residual silver. Figure 48 shows residual silver on the surface of the micropillars. Figure 49 shows a closer view. Certain areas had silver formed in dendrites as pictured in previous figures as well as Figure 49 and Figure 50. Others had silver form in films similar to Figure 41; Figure 48 and Figure 452 display this. For Trials 11, 12, and 13 displayed both areas of silver film and silver dendrites. The dendrites were scattered across the entire surface of the silicon nanowire surface, while the films were localized to different areas. As was the case with Trial 11 in Figure 47, the same behavior of silver sitting atop the nanowire structures is pictured in Figures 50 and 51 (Trial 12) and Figures 53 and 54 (Trial 13).

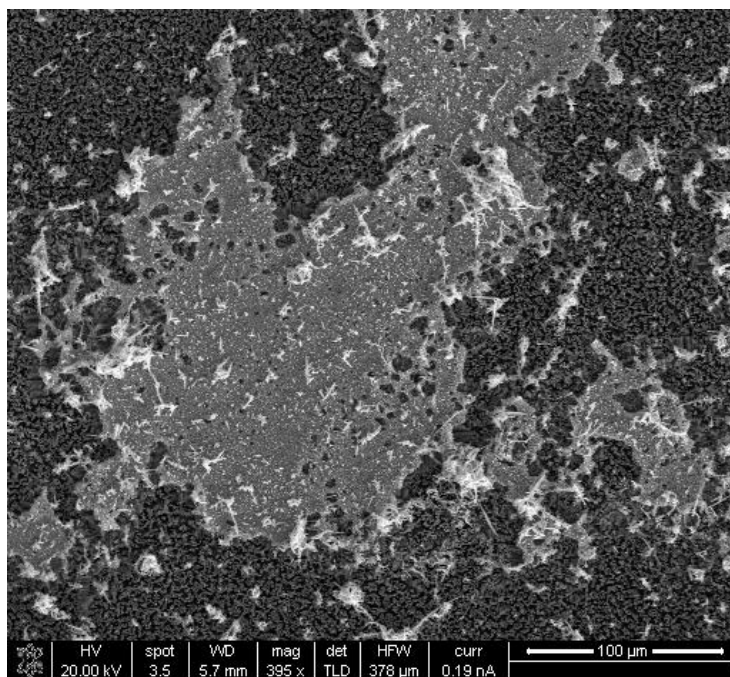


Figure 48: Trial 12, 8.15 M HF, 0.02 M AgNO₃, top down view

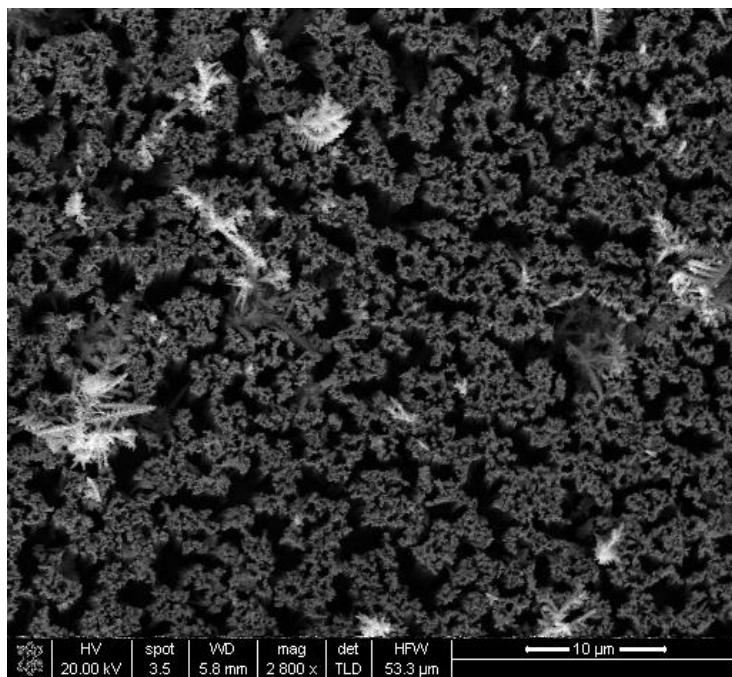


Figure 49: Trial 12, 8.15 M HF, 0.02 M AgNO₃, top down view

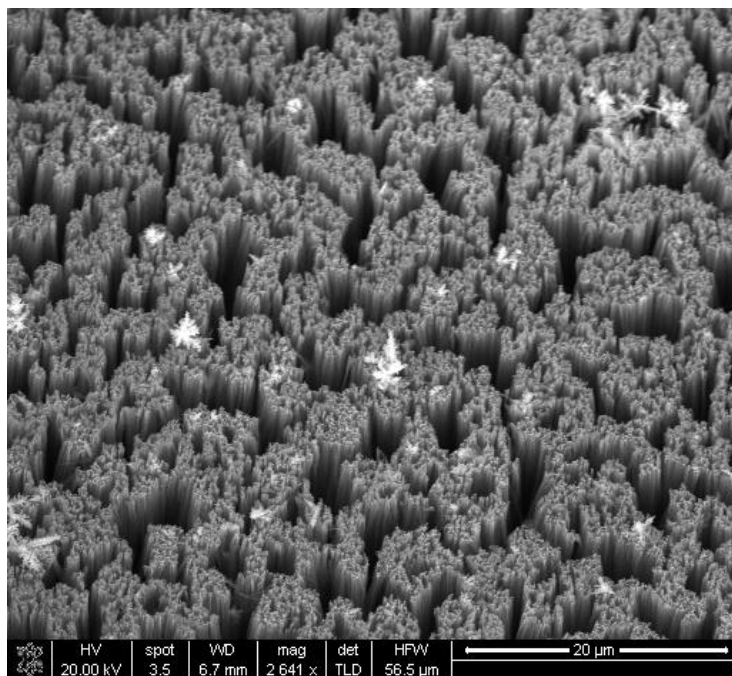


Figure 50: Trial 12, 8.15 M HF, 0.02 M AgNO₃, 20° tilt view

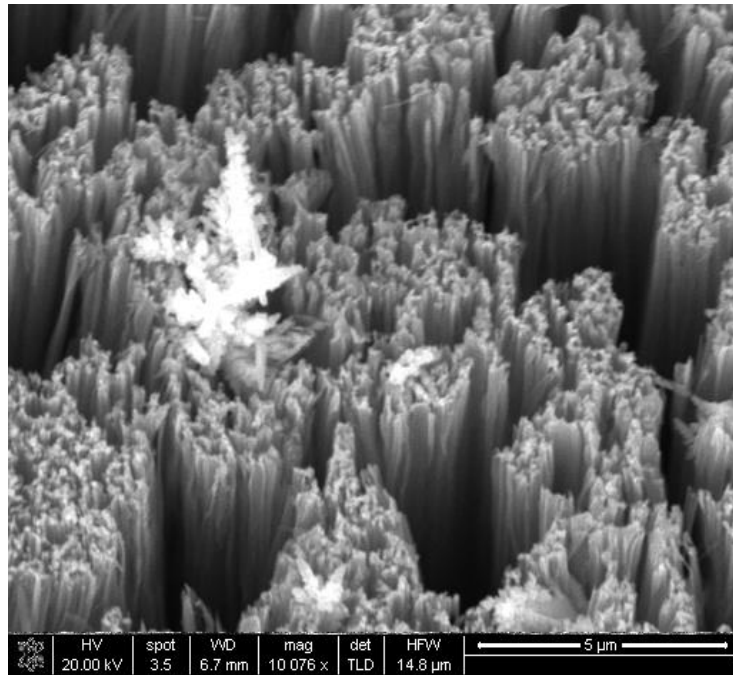


Figure 51: Trial 12, 8.15 M HF, 0.02 M AgNO₃, 20° tilt view

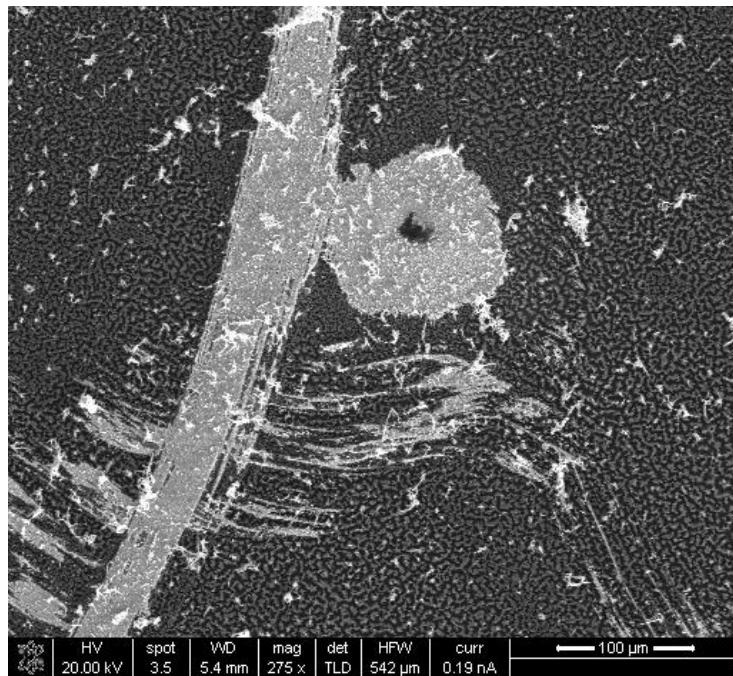


Figure 52: Trial 13, 12.2 M HF, 0.02 M AgNO₃, top down view

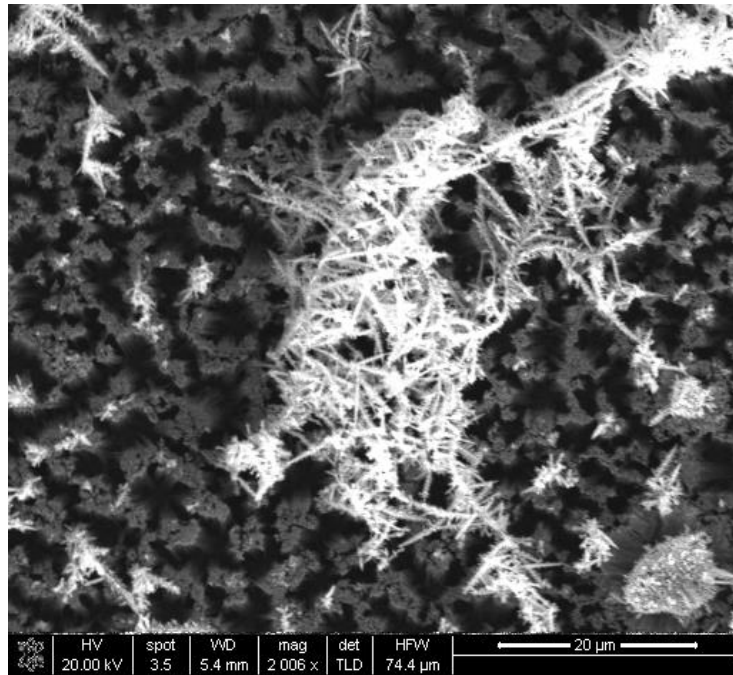


Figure 53: Trial 13, 12.2 M HF, 0.02 M AgNO₃, top down view

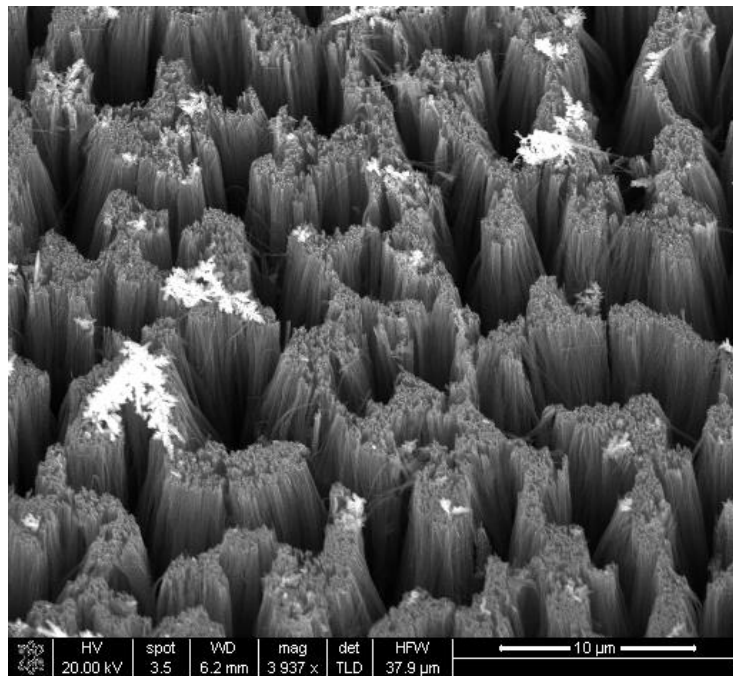


Figure 54: Trial 13, 12.2 M HF, 0.02 M AgNO₃, 20° tilt view

Figures 55 through 59 show images of Trials 7, 8, and 9 after having silver sputtered onto the surface. Visually it appears little to no silver was deposited onto the surface; however, it is believed there is silver there due to the presence of silver adjacent to the chip on the glass slide during the sputtering process. Raman spectroscopy results in Section E also indicate the presence of silver due to the increased signal strength.

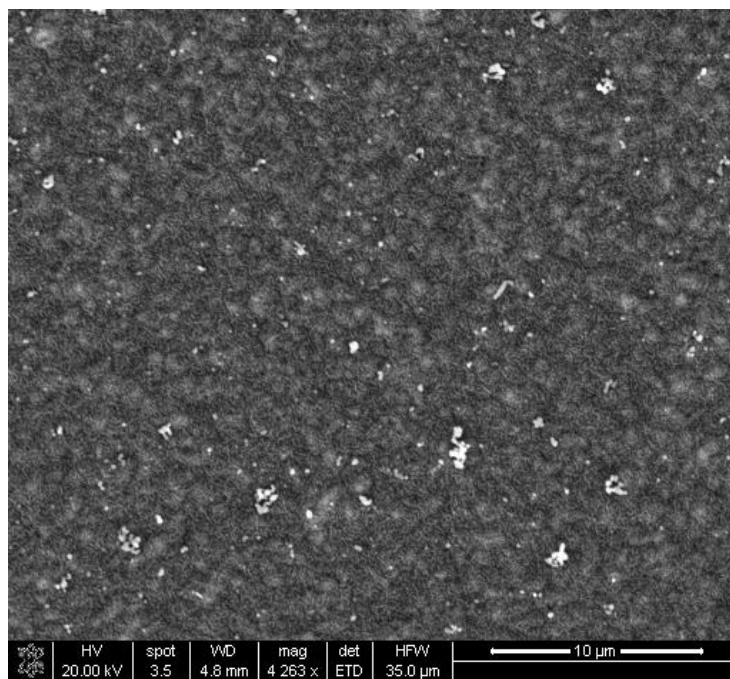


Figure 55: Trial 7, 2 M HF, 0.02 M AgNO_3 , sputtered Ag top down view

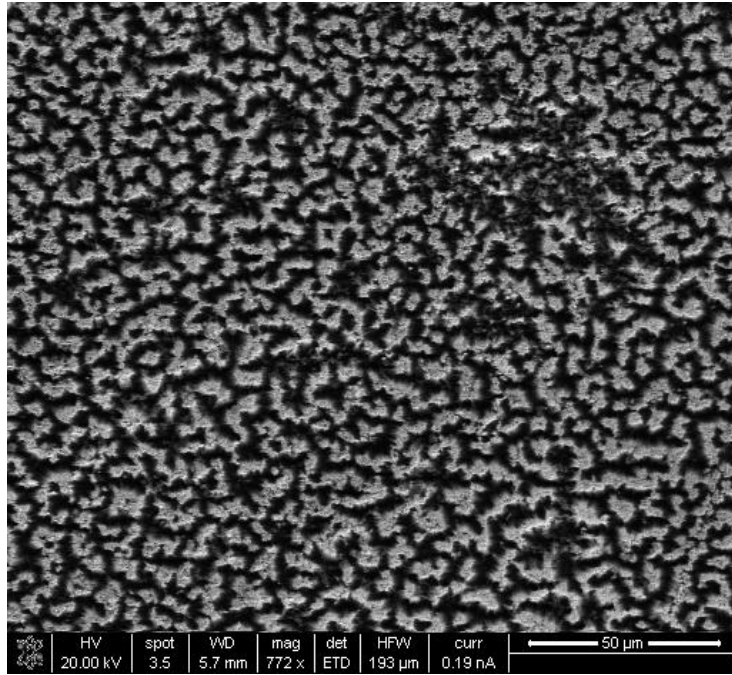


Figure 56: Trial 8, 8.15 M HF, 0.02 M AgNO_3 , sputtered Ag top down view

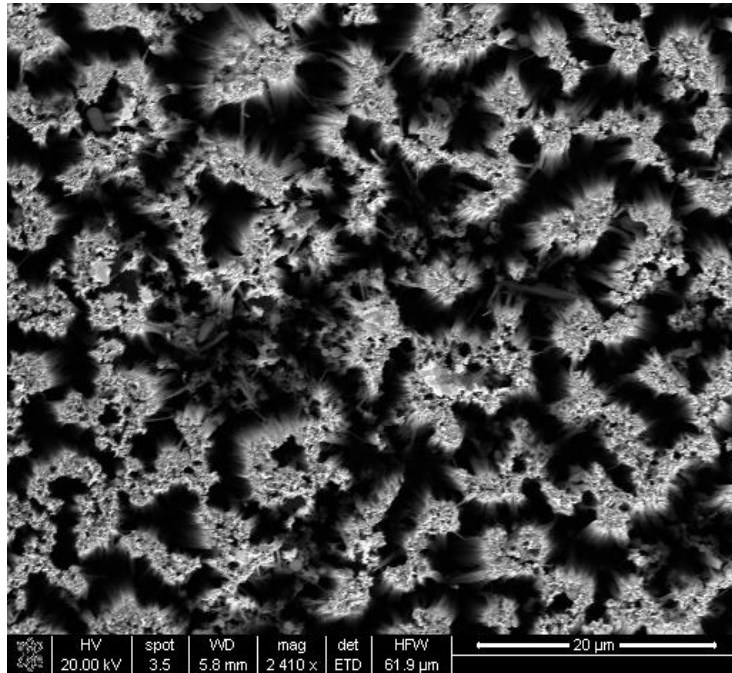


Figure 57: Trial 8, 8.15 M HF, 0.02 M AgNO_3 , sputtered Ag top down view

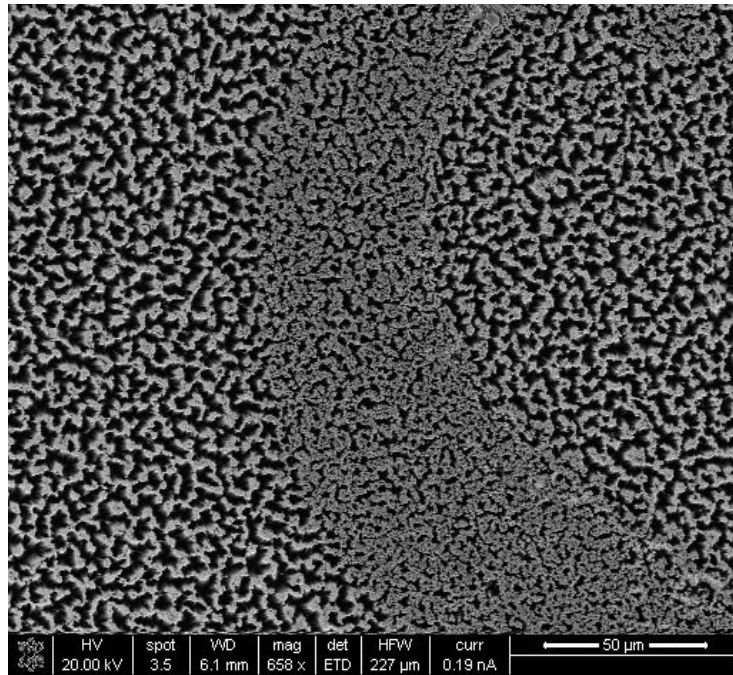


Figure 58: Trial 9, 12.2 M HF, 0.02 M AgNO_3 , sputtered Ag top down view

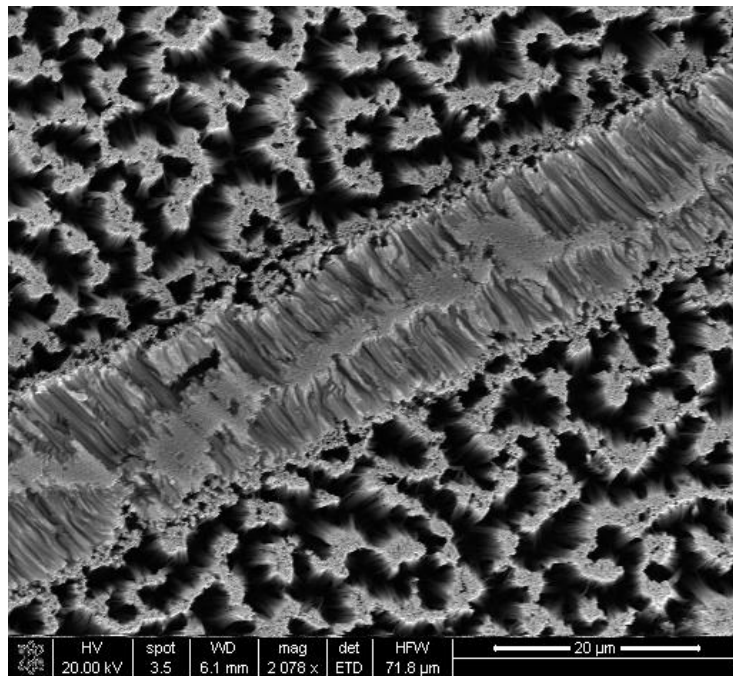


Figure 59: Trial 9, 12.2 M HF, 0.02 M AgNO_3 , sputtered Ag top down view

of the deposition layer while the deposition time was kept at 1 minute. The resulting profilometer reading was roughly 35 nm, pictured in Figure 61.

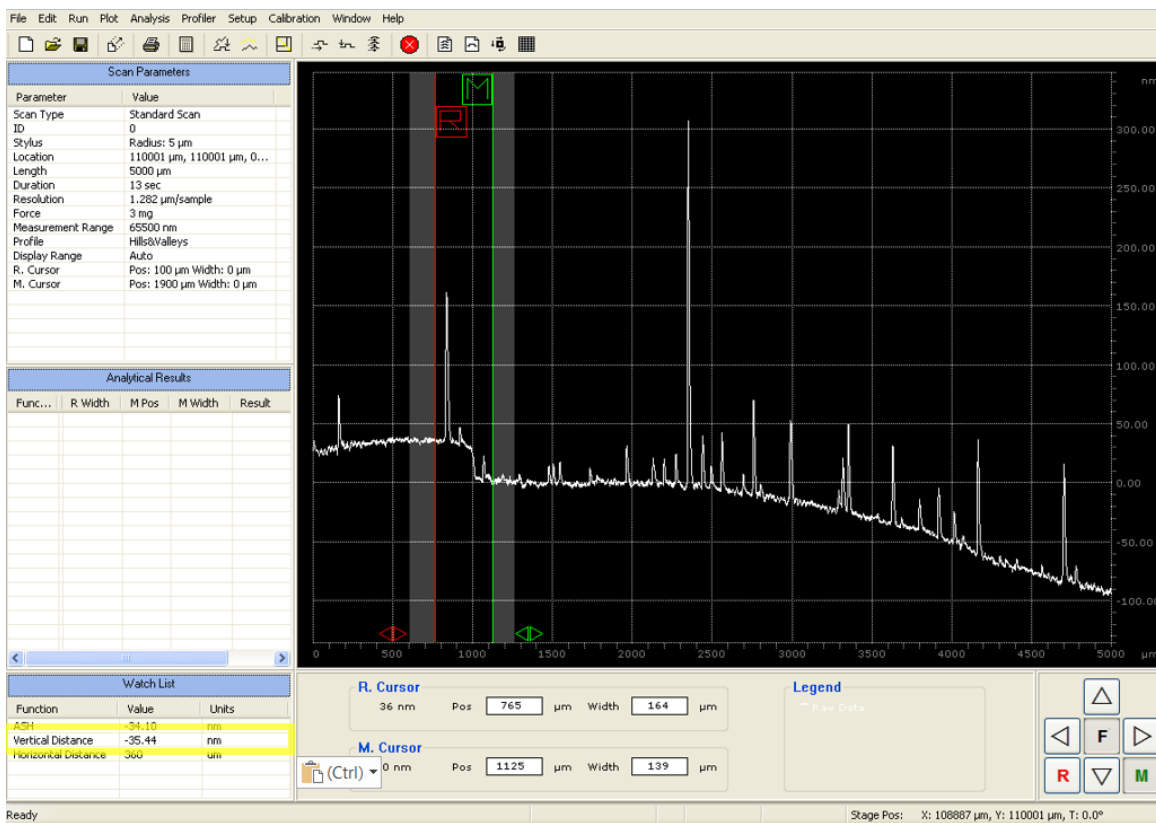


Figure 61: Profilometer measurement, 150 W power, 60 minute pump time, 1 minute deposition time

To decrease the sputtering thickness further, deposition time was lowered to 30 seconds while power remained at 150 W and pump time remained at 60 minutes. The resulting silver layer thickness was roughly 21 nm and is pictured in Figure 62. It was deemed that these sputtering conditions could be suitable for SERS activity and were used in all trials moving forward.

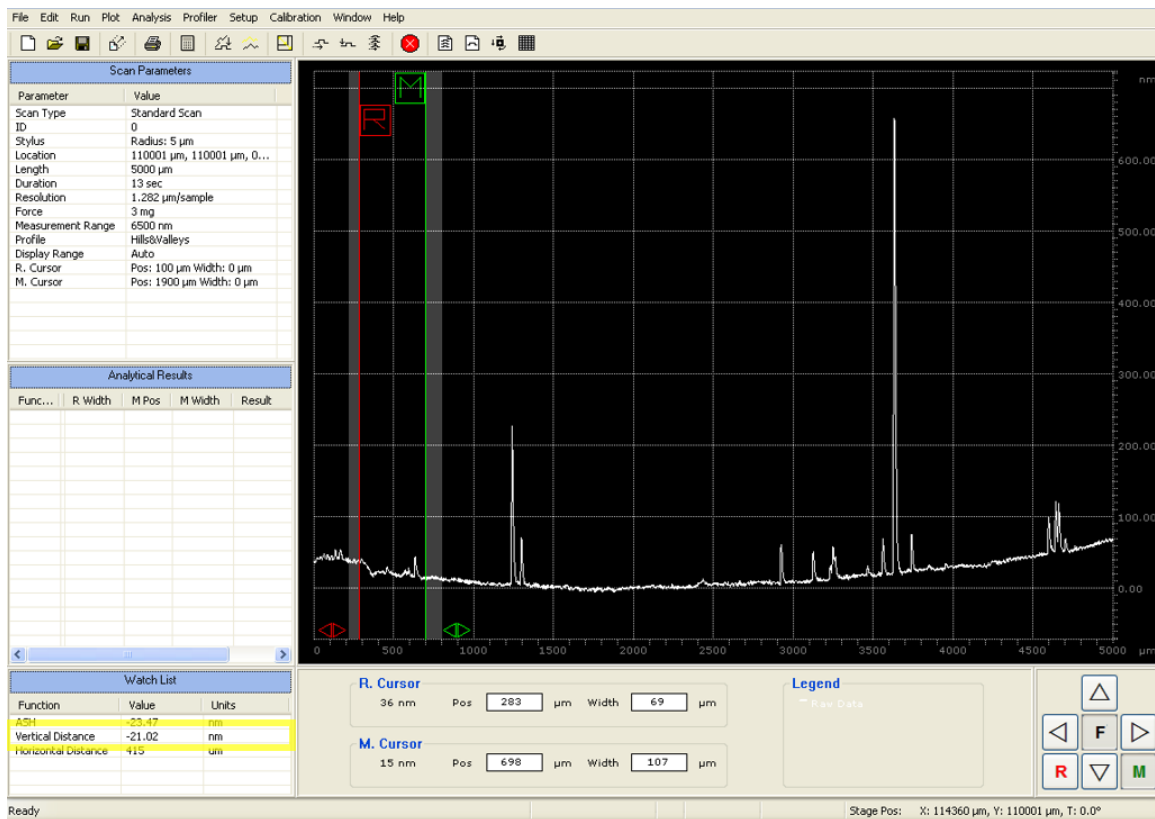


Figure 62: Profilometer measurement, 150 W power, 60 minute pump time, 30 second deposition time

D. RAMAN SPECTROSCOPY RESULTS

A stock solution of 1.0 mg/mL of (-)-trans- Δ^9 -THC in methanol solution was the analyte for Raman spectroscopy. The first attempts to detect THC were qualitative in nature; it was desired to show the silver sputtered, etched silicon chips could provide enough signal enhancement to detect trace amounts of THC. As reported by Yüksel et al. (2016), the characteristic peak for THC is at 1390 cm^{-1} . 10 μL of the THC solution was deposited onto a bare (unetched) silicon chip and the resulting measurements are displayed in Figure 63. 10 μL (equal to 1.0×10^7 pg) was chosen as the starting point because it is significantly higher than the amount of THC typically found in exhaled breath (1479 pg for the case of Coucke et al., 2016). There is a strong peak intensity at

590 cm^{-1} , corresponding to silicon. The lack of response at 1390 cm^{-1} evident in Figure 63 shows that unetched silicon has no SERS activity.

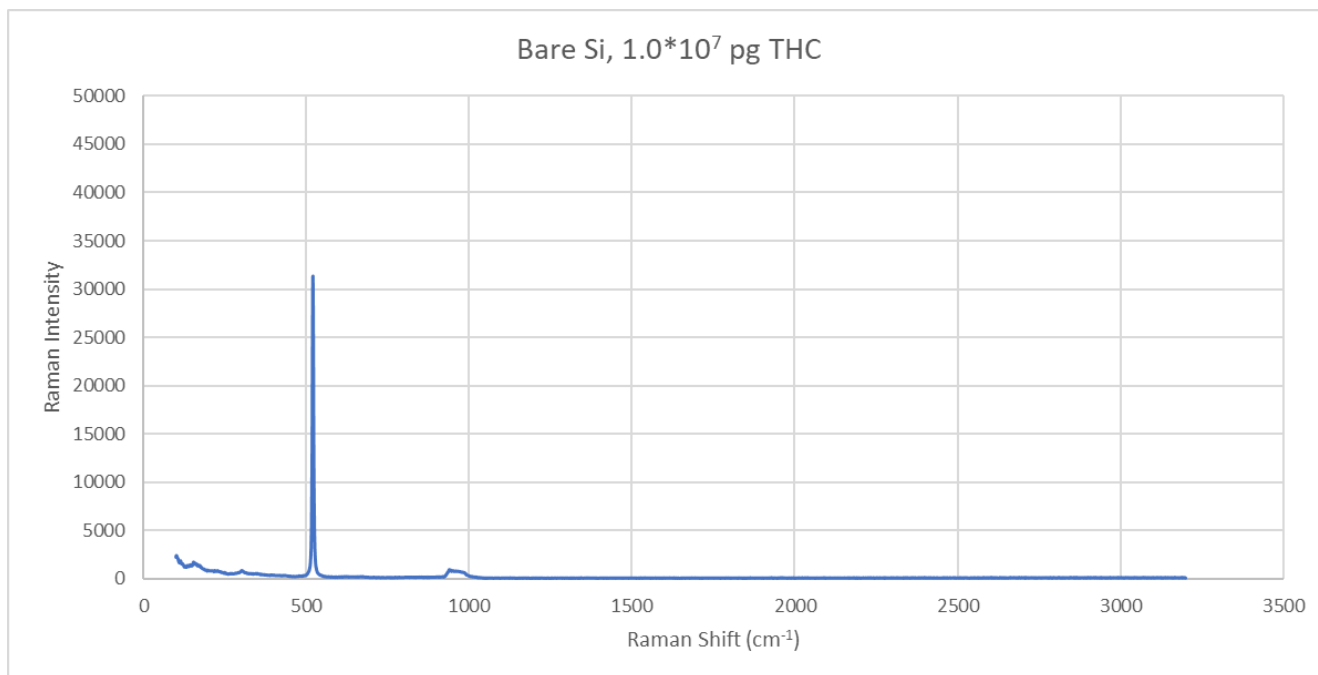


Figure 63: 10 μL (1.0×10^7 pg) of THC on bare Si

THC on a bare, unetched silicon with a film of silver sputtered on was also measured. Figure 64 displays the result. The response intensity was minimal, indicating unetched silicon and sputtered silver do not provide any Raman enhancement. As silver is not Raman active, no strong peaks are present. The film of silver covering the entire surface likely obstructed silicon enough to prevent the silicon peak from registering.



Figure 64: Bare Si chip, 10 μL (1.0×10^7 pg) of THC on bare Si with Ag sputtered on

The silicon chip etched in 2 M HF, 0.02 M AgNO₃ solution (Trial 7) was tested with 1006 pg of THC. It was theorized that due to the lack of micropillar structures shown in the SEM image (Figure 31) that there would be limited SERS activity. Figure 65 confirmed this hypothesis. With 1006 pg of THC, no Raman activity was detected (outside of silicon).

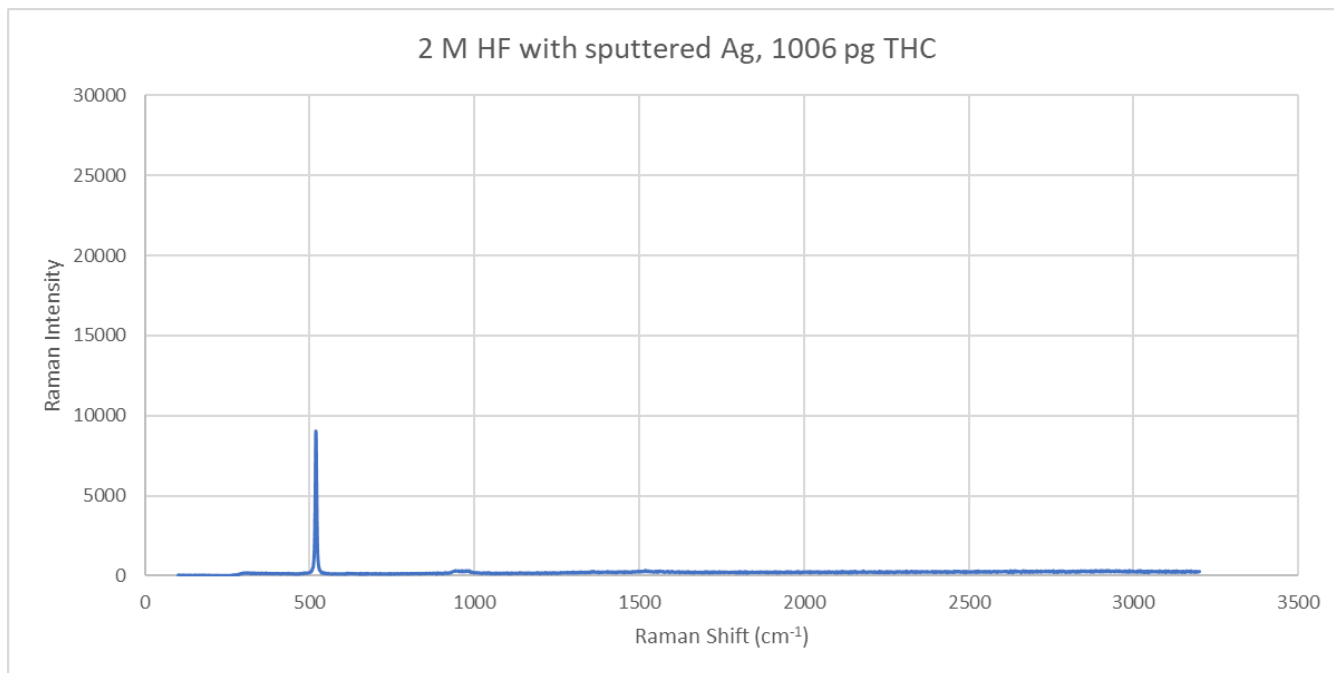


Figure 65: Trial 7 chip, 2 M HF, 0.02 M AgNO₃ solution, 1006 pg of THC

The lack of etching displayed in the SEM images of Trial 7 combined with the no THC spectra displayed led to no further pursuit of the 2 M HF etching parameter chip. The remaining Raman trials focused on Trials 8, 9, 10, 11, and 12. Trial 10 and Trial 11 used 5 M HF solution and were utilized to investigate the potential of using residual from the HF/AgNO₃ etch as a SERS mechanism. Figure 65 and Figure 66 display a dramatic difference in signal on the same chip. The Trial 11 chip was etched with a 5 M HF and 0.1 M AgNO₃ solution and the residual silver was left on the surface. Figure 65 shows the spectral response of THC on an area with no residual silver, while Figure 66 shows the response on an area with residual silver on the nanowires.

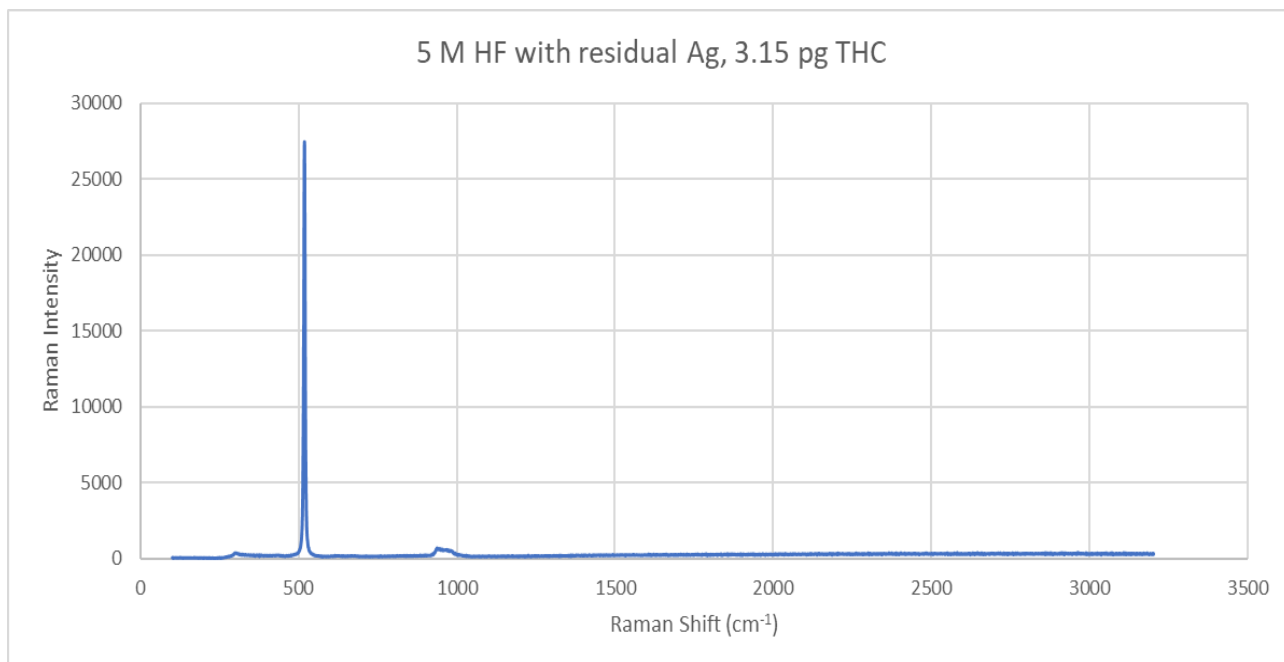


Figure 65: Trial 11, 5 M HF, 0.02 M AgNO₃, 3.15 pg THC over no residual Ag

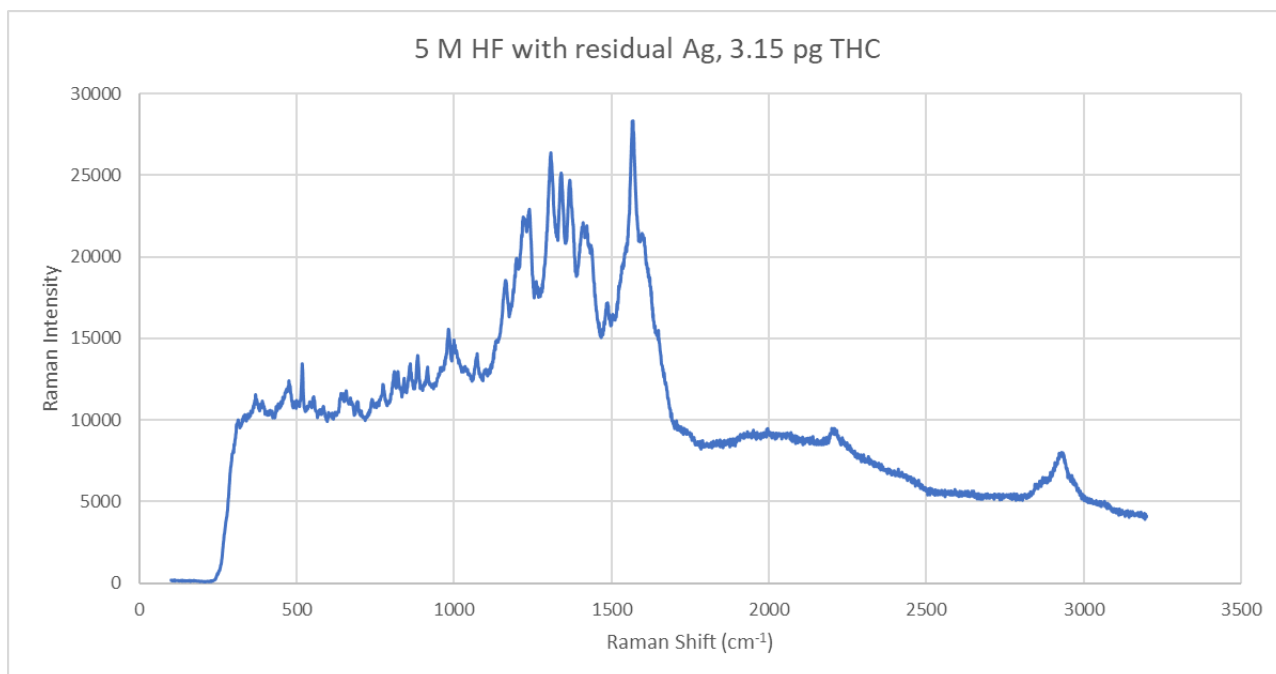


Figure 66: Trial 11, 5 M HF, 0.02 M AgNO₃, 3.15 pg THC over residual Ag

3.15 pg was chosen as the amount for analysis due to it being well below the upper limit found in breath after consumption of THC by inhalation. Even though Figure 65 and Figure 66 measurements were taken on the same chip, the spectral responses are completely different. The spectral responses indicate silver is necessary for Raman enhancement. Being able to rely on residual silver for signal enhancement would have been advantageous due to eliminating the need for sputtering equipment. However, the sparse and irregular distribution of residual silver ruled out relying on it for signal enhancement. While there is signal response in Figure 66 for THC, located at 1390 cm^{-1} with an intensity of 18,876, the surrounding peaks and background noise are a concern for quantification. But qualitatively, it appears Trial 11 conditions can detect a THC response with 3.15 pg of analyte.

Trial 10 was performed to determine if increasing the silver concentration would leave more residual silver and thus eliminate need the need for sputtering. The etch parameters were the same as Trail 11, but with 0.10 M AgNO_3 in the etching solution instead of 0.02 M. Figure 41 shows the SEM results of Trail 10 and Figure 67 shows the spectral response. The SEM images show a silver particle film across the surface of the chip, obscuring the nanowires beneath. The lack of a spectral response other than silicon suggest the nanowires need to be exposed for Raman signal enhancement to occur.

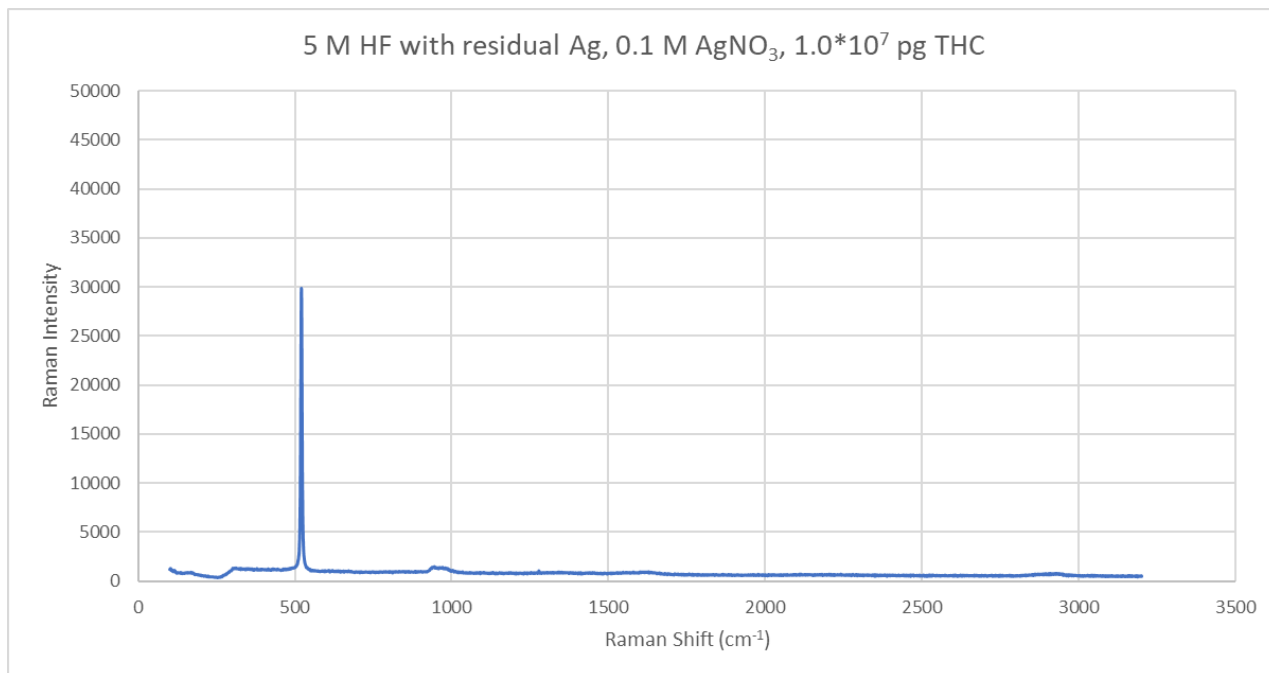


Figure 67: Trial 10, 10 μL (1.0×10^7 pg) of THC on Si chip etched with 5 M HF/0.10 M AgNO₃ with residual Ag

Thus far, it has been shown that silver particles enhance signal for THC detection while silver films and particle films provide no enhancement capabilities. The results also suggest the necessity of nanowires to provide enhancement, with the poorly etched Trial 7 chip not displaying signal and the Trial 10 chip not displaying signal due to the nanowires being obstructed by silver. Next, Trial 8 (8.15 M HF/0.02 M AgNO₃ with sputtered silver) and Trial 12 (8.15 M HF/0.02 M AgNO₃ with residual silver) were investigated. SEM images taken before sputtering on the Trial 8 chip are shown in Figure 35 through Figure 37. The presence of defined nanowires indicates a successful etch and the potential for SERS activity once silver was deposited. The SEMS images in Figures 56 and 57 are of the Trail 8 chip after being sputtered. While no silver is blatantly visible in the images, it is believed that silver is present on the pillars. This conclusion is based on the

presence of silver adjacent to the chip after sputtering as well as the signal enhancement displayed in Figure 68. Figure 68 shows the sputtered Trial 8 chip signal response.

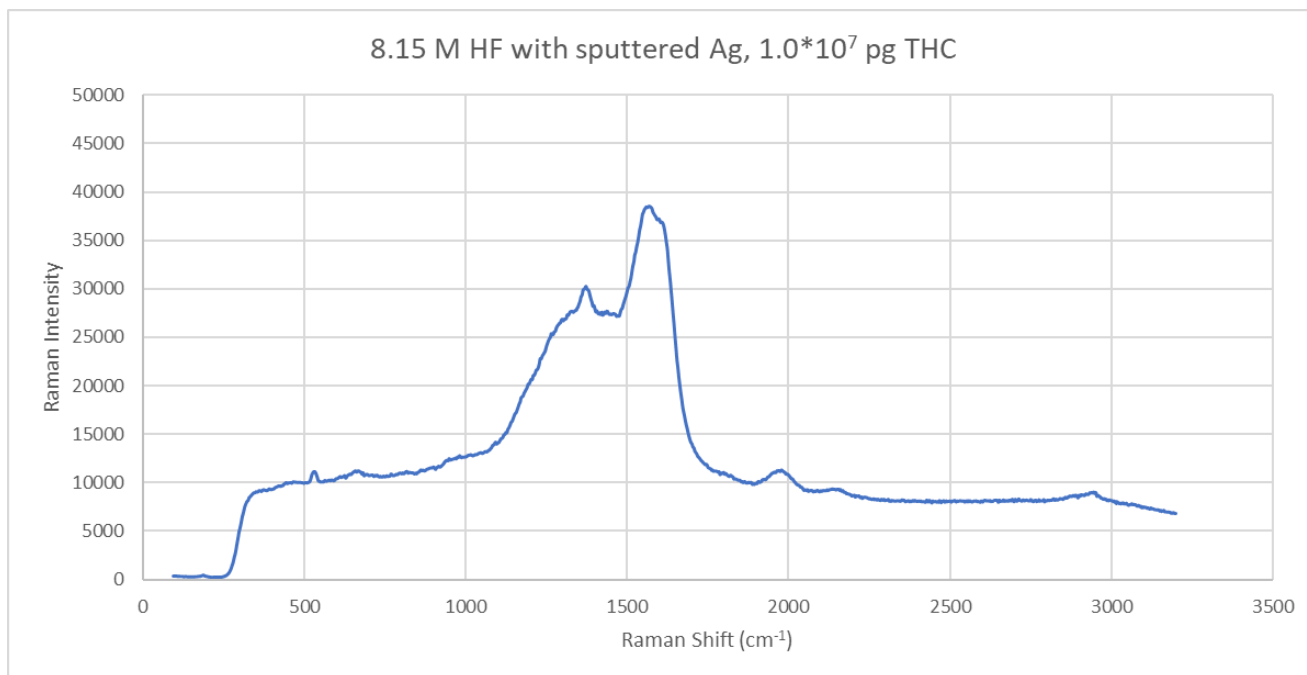


Figure 65: Trial 8, 10 μL ($1.0 \cdot 10^7$ pg) of THC on Si chip etched with 8.15 M HF/0.02 M AgNO_3 with sputtered silver

While there is background noise for the signal on the level of 8000 and the peaks are not sharp and defined, there is still a noticeable response at 1390 cm^{-1} of 28,586. It can be concluded from this that Trial 8 etching conditions and silver sputtering allow for qualitative detection of THC. Trial 12 with residual silver was tested with 3.15 pg of THC. The measurement in Figure 69 was taken over an area with no residual silver visible while Figure 70 was measured over residual silver.

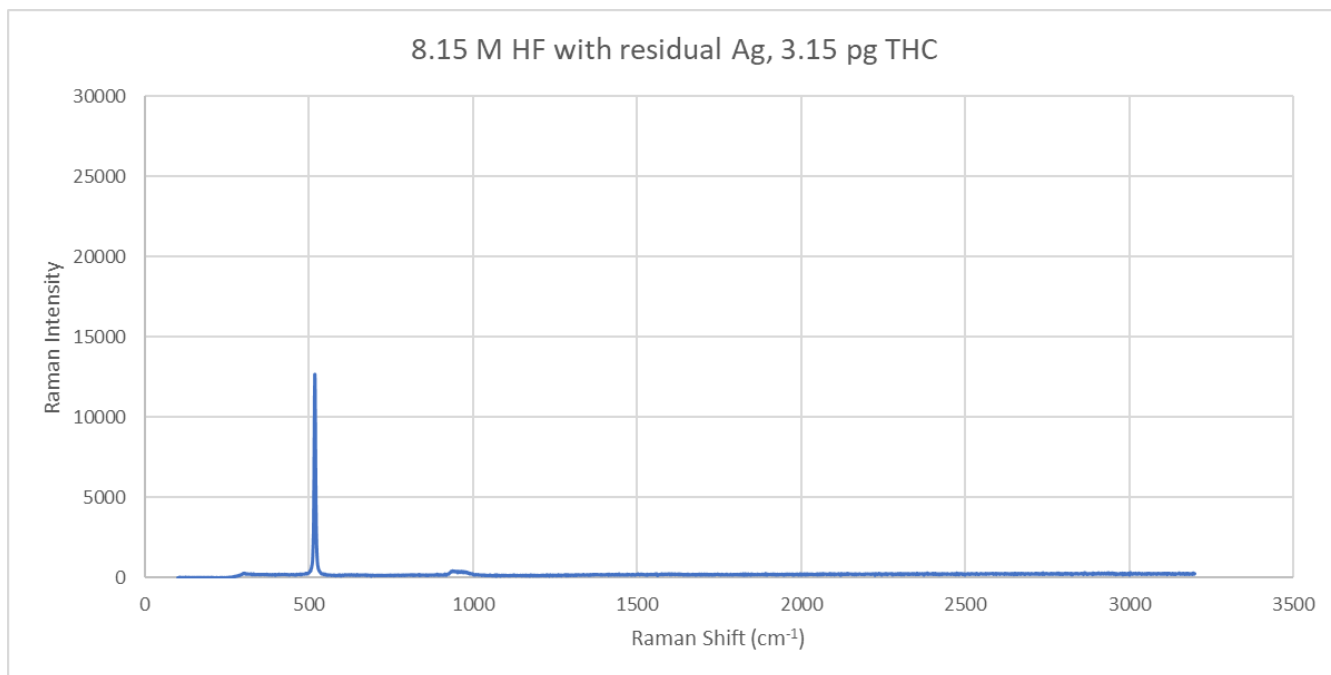


Figure 69: Trial 12, 3.15 pg of THC on Si chip etched with 8.15 M HF/0.02 M AgNO₃ with residual silver, measurement over no silver area on chip

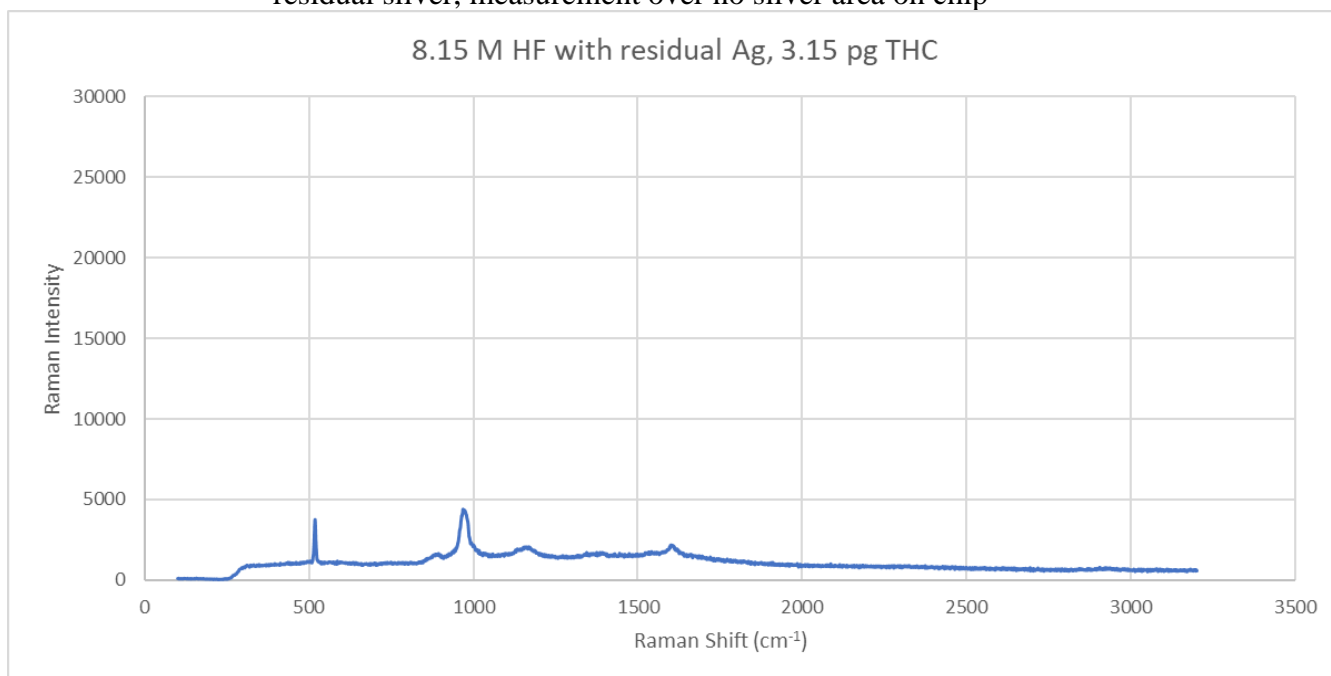


Figure 70: Trial 12, 3.15 pg of THC on Si chip etched with 8.15 M HF/0.02 M AgNO₃ with residual silver, measurement over silver on chip

Much like Figure 65 (Trial 11), Figure 69 displays no spectral response for THC. This is to be expected because the measurement was taken over in an area with no silver. Without silver, signal enhancement is not possible in these circumstances. However, it is unexpected that Figure 70 displays little signal enhancement. With Figure 66 (Trial 11) displaying a spectral response at the THC wavelength, it was hypothesized that signal enhancement would occur for Trial 12 as well. It was initially thought the etching parameter was not conducive to SERS activity, but later measurements with Trial 9 and Trial 13 (etching parameters of 12.2 M HF/0.02 M AgNO₃) display spectral response with 3.15 pg THC. With trials at 5M HF and 12.2 M HF both displaying SERS activity while 8.15 M HF did not, it is thought that the 8.15 M HF chip measurements over silver may have been on a conglomerate of silver. The lack of response is similar to Figure 67, where silver covered the micropillar pillars. Perhaps if the measurement for Figure 70 had been over an area with slightly less silver, a spectral response for THC would have been observed.

Figure 71 shows the results from measuring 10 μ L (1.0 X 10⁷ pg) on Trial 9 ((etching parameters of 12.2 M HF/0.02 M AgNO₃ with sputtered silver). The spectral response is similar in pattern to the Trial 8 counterpart in Figure 68, albeit with a peak of lower intensity (with a value of 15,248) at 1390 cm⁻¹ and with less definition. Signal enhancement is there, but it is difficult to identify THC specifically due to the lack of peak definition.

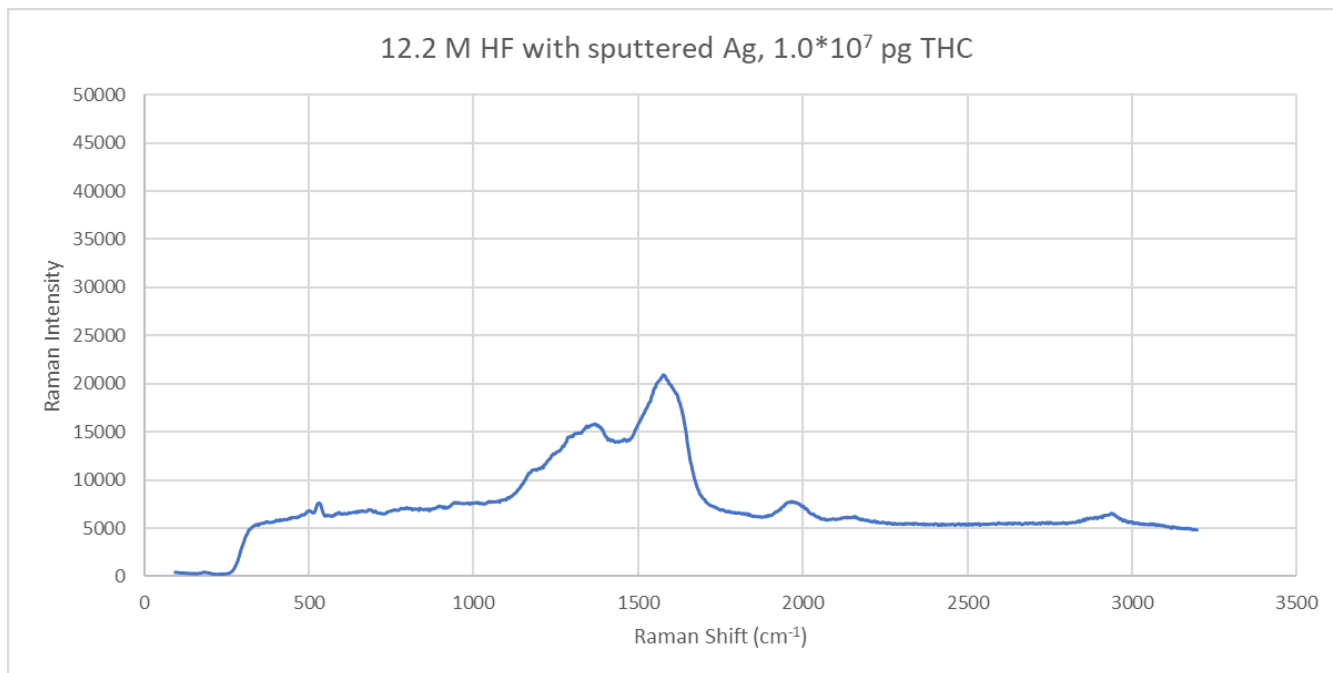


Figure 71: Trial 9, 10 μL (1.0×10^7 pg) of THC on Si chip etched with 12.2 M HF/0.02 M AgNO_3 with sputtered silver

Figure 72 (Trial 13, 12.2 M HF/0.02 M AgNO_3 with residual silver, measurement over no silver area on chip) and Figure 73 (Trial 13, 12.2 M HF/0.02 M AgNO_3 with residual silver, measurement over silver on chip) show results with 3.15 pg on the chips. Figure 72 again confirms that even with micropillars, if there is no silver present, signal enhancement does not occur. The measurement shown in Figure 73 takes place over an area with residual silver and displays a spectral response. At the THC wavelength of 1390 cm^{-1} the response intensity is 7075. When comparing Figure 72 to Figure 73, it can be concluded that when measured over residual silver, Trial 13 etching conditions are able to qualitatively detect THC.

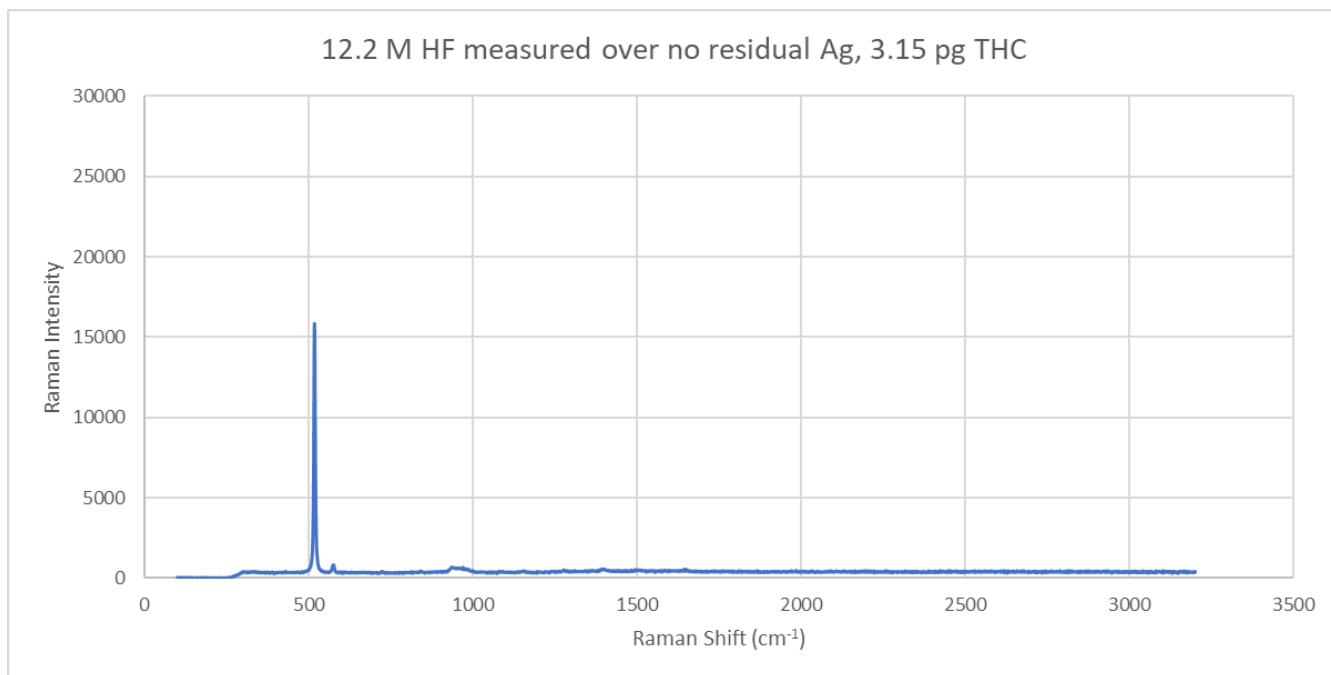


Figure 72: Trial 13, 3.15 pg of THC on Si chip etched with 12.2 M HF/0.02 M AgNO₃ with residual silver, measurement over no silver area on chip

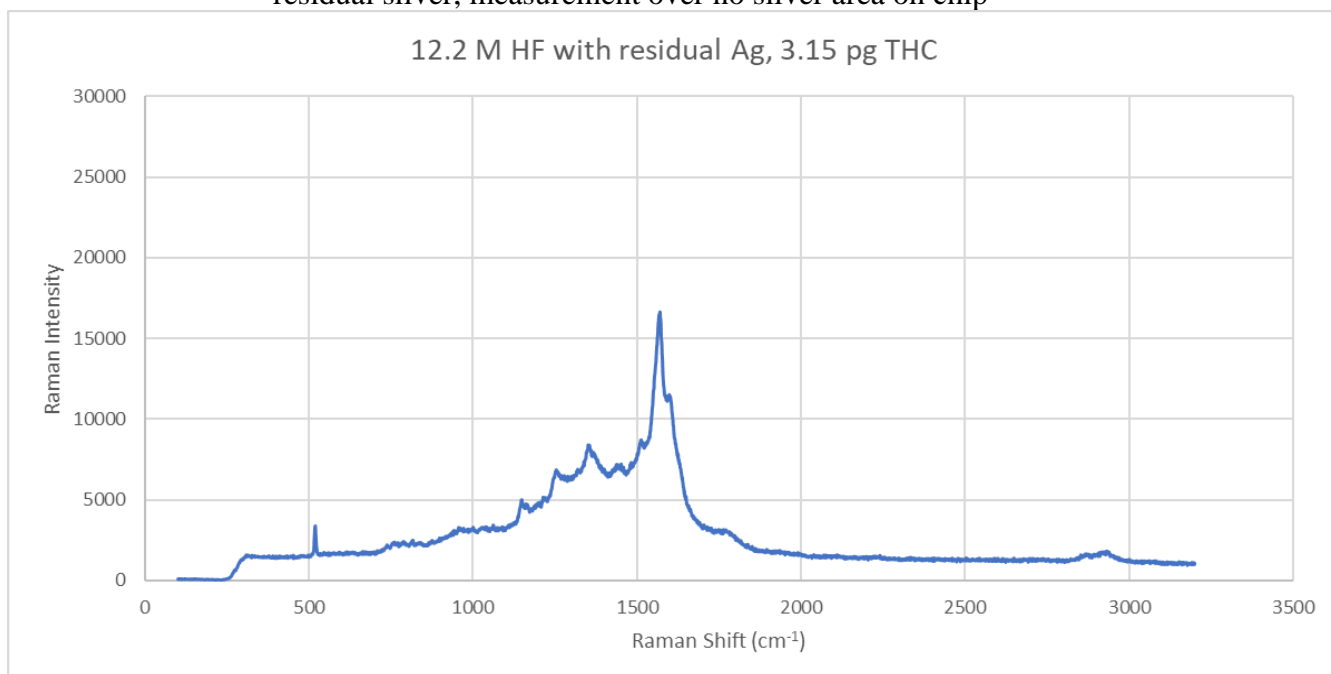


Figure 73: Trial 13, 3.15 pg of THC on Si chip etched with 12.2 M HF/0.02 M AgNO₃ with residual silver, measurement over no silver area on chip

After performing qualitative tests for the detection of THC, a quantitative test was performed. The Trial 8 chip conditions (8.15 M HF, 0.02 M AgNO₃ etching solution) with sputtered silver was chosen as the substrate for this test due to it having the highest intensity spectral response of the tested chips. The quantitative test was not performed with chips utilizing residual silver due to the variability of measurement output from location on the chip (i.e. whether the measurement was over residual silver or not).

Various amounts of THC were tested for spectral response. One challenge to this step was the amount of background noise for the measurements. As can be seen in several of the previous figures in this work (such as Figure 66, Figure 68, Figure 71, and Figure 73) there is a certain level of background noise for the measurements. For quantitative analysis, the background noise was taken into account by subtracting the baseline from the response intensity for each amount of THC. For one set of data the baseline of the response was set to a flat section from the first half of the data (between 600 cm⁻¹ and 800 cm⁻¹). For the other set of data, the second half with a flat response was set as the baseline (between 2000 cm⁻¹ and 3000 cm⁻¹). The responses are shown in Figure 74 and Figure 76. Calibration curves based on the response intensity at 1390 cm⁻¹ are shown in Figure 75 and Figure 77.

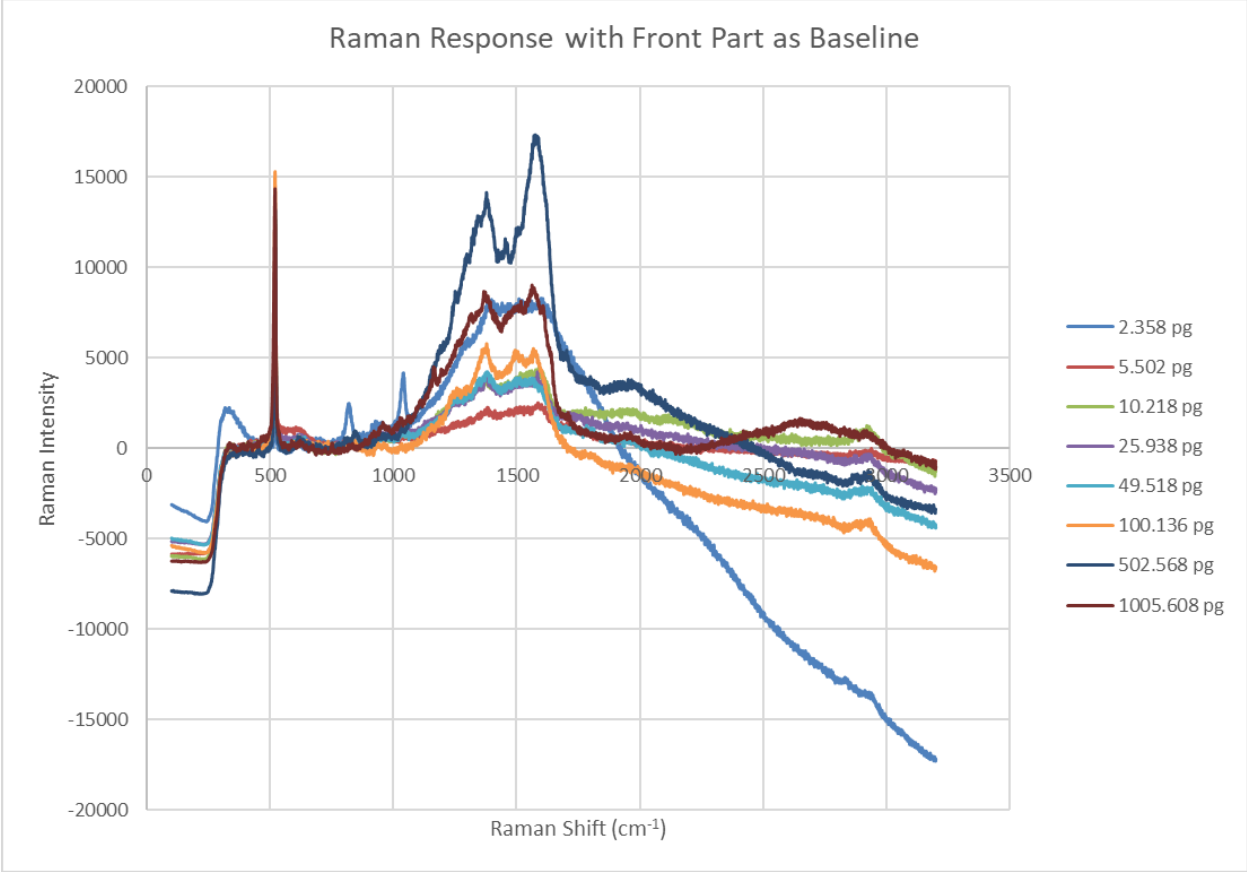


Figure 74: Raman response to various amounts of THC using the front part of the data as a baseline

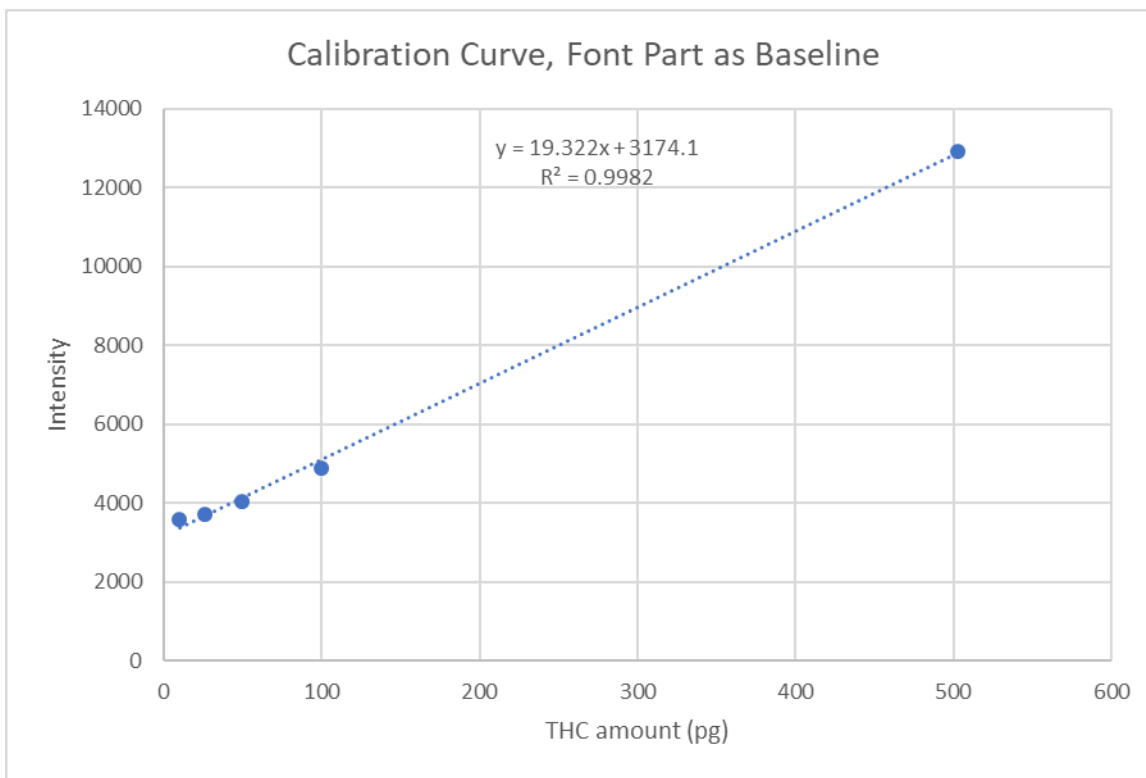


Figure 75: Calibration curve from the response intensity at 1390 cm^{-1} from Figure 71

The intensity values from at 1390 cm^{-1} from Figure 74 are displayed in Table 7. The highlighted values were used to generate the calibration curve in Figure 75. The highlighted values were chosen because the associated linear regression proved to have an R^2 value close to 1. The remaining three values were deemed outliers and not used for the regression. However, the outliers do raise the question of reliability of this method for identifying different amounts of THC.

Table 7: Intensity at 1390 cm⁻¹ for Varying Amounts of THC (for Figure 72)

THC amount (pg)	Intensity
2.358	8098.65
5.502	2098.56
10.218	3586.53
25.938	3727.46
49.518	4051.9
100.136	4872.97
502.568	12932.6
1005.608	7983.5

Figure 76 shows the spectral response with the tail part of the data acting as the baseline. Figure 77 shows the associated calibration curve, and Table 8 contains the associated data points for signal intensity at 1390 cm⁻¹ in response to varying amounts of THC. The calibration curve in Figure 77 generated from the Raman response in Figure 76 is not as good of a fit as the calibration curve in Figure 75, with a lower R² value of 0.8728. Inconsistency between the front part as baseline and the tail part as baseline measurements leads to the conclusion that further work is necessary in order to develop this method as a reliable method for THC quantification. However, these initial results indicate promise in the method with further refinement. It should also be noted a distinct peak was consistently present at ~1590 cm⁻¹. It is thought this peak corresponds to a potential overlap in methanol and THC response. This is supported by a similar response seen by Yüksel et al (2016). However, the intensity of the peak seen in the presented work is perplexing and deserves further investigation.

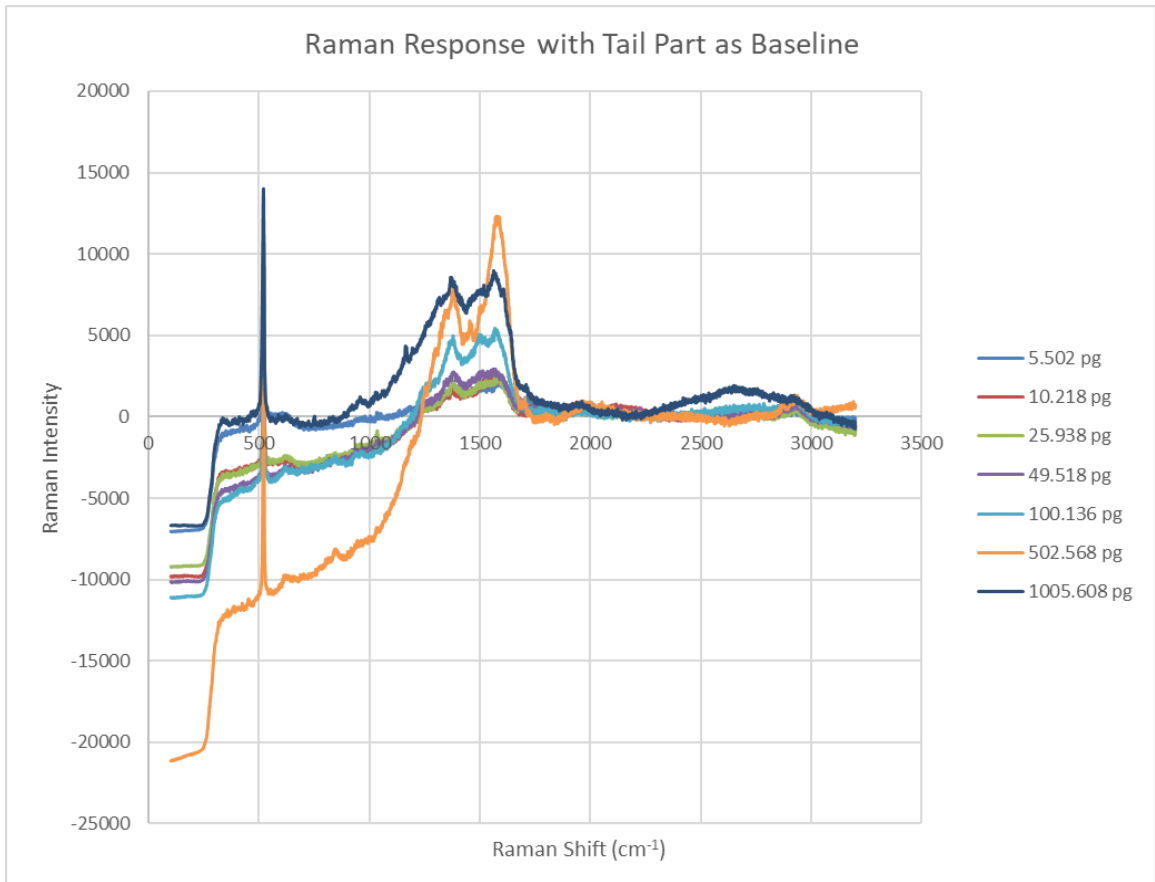


Figure 76: Raman response to various amounts of THC using the tail part of the data as a baseline

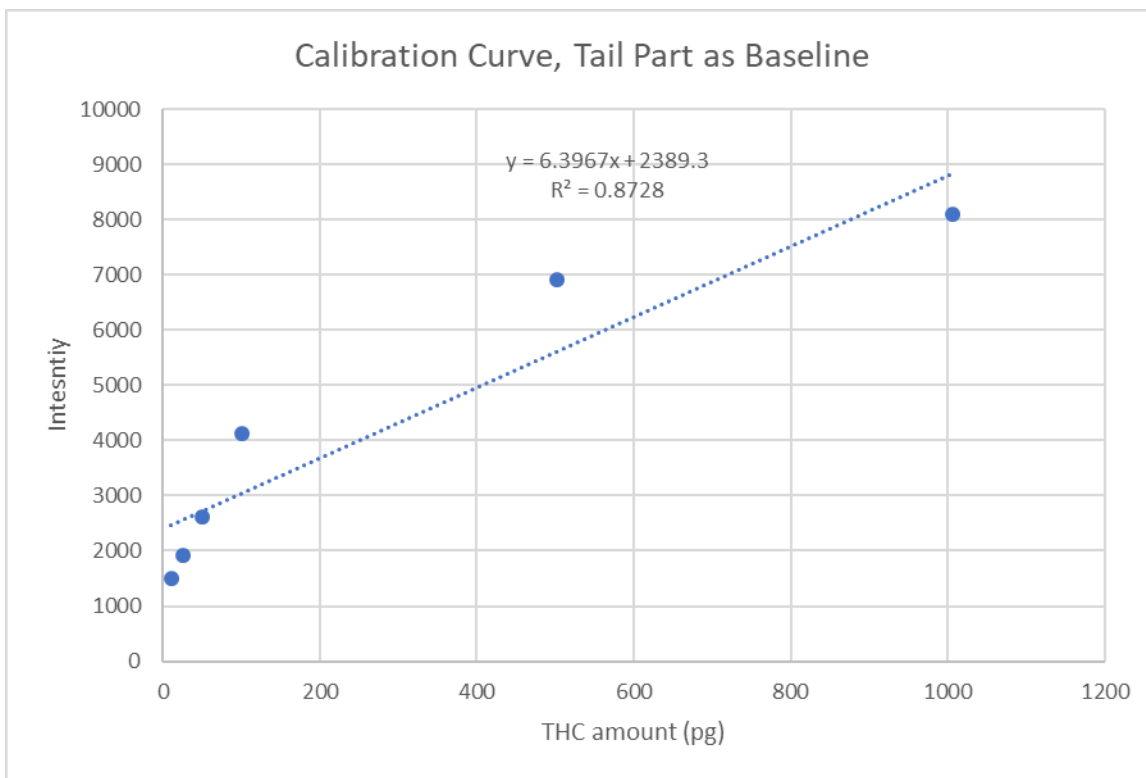


Figure 77: Calibration curve from the response intensity at 1390 cm^{-1} from Figure 73

Table 8: Intensity at 1390 cm^{-1} for Varying Amounts of THC (for Figure 74)

THC amount (pg)	Intensity
5.502	1667.03
10.218	1501.23
25.938	1925.71
49.518	2613.49
100.136	4132.09
502.568	6908.05
1005.608	8090.77

V. CONCLUSION

The main objective presented in this work was to produce a microfabricated SERS platform for the detection of tetrahydrocannabinol (THC). It was desired to utilize silicon micropillars as the substrate with deposited silver acting as a mechanism for Raman enhancement. The work initially focused on utilizing photolithography to create the substrate, but the focus shifted to utilizing wet etching once cost considerations and equipment limitations came into consideration. A solution of hydrofluoric acid (HF) and silver nitrate (AgNO_3) was used to etch silicon nanowires to serve as a SERS substrate. Various concentrations of HF were investigated to create an optimal substrate for SERS. With AgNO_3 held constant at 0.02 M, etching was performed at 2 M, 5 M, 8.15 M, and 12.2 M HF. A scanning electron microscope was used to view the results of silicon etching. 2 M HF failed to etch while 5 M, 8.15 M, and 12.2 M HF etched and produced nanowires. An increase of AgNO_3 concentration to 0.10 M was tried with 5 M HF; it left a film of silver particles on the surface of the chip, obstructing nanowires. When the silicon chips were not cleaned of residual silver with a nitric acid wash, residual silver was seen on the micropillars. For chips that were cleaned, sputtering was used to deposit silver. Sputtering conditions of 150 W power, 60-minute pump time, 30 second deposition time created a ~20 nm thick layer of silver and was determined to suitable for the investigation as the silver didn't obstruct the nanowires. Raman

spectroscopy measurements were taken to qualitatively detect THC. It was proven bare silicon provides no signal enhancement, either with or without deposited silver.

For the different concentrations of HF, measurements were taken with residual silver from the etch serving as the source of enhancement. At 5 M HF/0.02 M AgNO₃, it was seen that nanowires with residual silver can detect a THC response at 1390 cm⁻¹ from 3.15 pg. However, residual silver proved to be sparsely distributed on the chips, and measurements in areas with no residual silver showed no signs of enhancement. This was confirmed at etching conditions of 8.15 M/0.02 M AgNO₃ and 12.2 M/0.02 M AgNO₃ for 3.15 pg as well. Measurements taken with sputtered silver at etching conditions of 8.15 M/0.02 M AgNO₃ and 12.2 M/0.02 M AgNO₃ showed a spectral response at 1390 cm⁻¹, indicating the presence of THC. The 8.15 M HF condition had a more intense response than 12.2 M (28,586 versus 15,248, respectively) and thus was chosen as the conditions for quantitative investigation.

The quantitative analysis sought to work past background noise that was prevalent in measurements. Flat sections of the background noise were subtracted from sections of the data to try and filter out noise. The response intensity for various amounts of THC was taken at 1390 cm⁻¹ and graphed to create a calibration curve. With the front part of data taken as a baseline, the calibration curve was $y = 19.322x + 3174.1$ and an R² of 0.9982. With the tail part of the

response as the baseline, the calibration curve was $y = 6.3967x + 2389.3$ with an R^2 of 0.8728.

The variability between the two measurements combined with the need to filter out background noise and the nonlinearity of certain data points leads to the conclusion that further work is necessary to accurately quantify trace amounts of THC by this method.

VI. RECOMMENDATIONS

Further optimization of etching parameters could lead to stronger SERS activity. Five different etching conditions were investigated, leaving many possibilities for different parameters to potentially create better conditions for Raman enhancement. An interesting aspect about residual silver was noticed, with some residual silver leaving feather-like dendritic structures. It would be interesting to investigate if this unique silver structure could provide more enhancement than sputtered silver. Utilizing photolithography was investigated in this work for a time and could prove to be a viable alternative if the proper photomask could be obtained. Photolithography combined with deep reactive ion etching (DRIE) would be a worthwhile alternative to pursue because it does not involve handling dangerous hydrofluoric acid from wet etching. In this work, THC in methanol solution was deposited directly onto the silicon substrate and allowed to evaporate. Quantification proved to be a challenge in this thesis; future works could attempt to improve quantification by minimizing background noise in measurements. Future works should investigate simulated breath samples by allowing the spiking a sample bag of breath with the THC solution.

REFERENCES

Intro and Lit Review References

Aksak, Burak, Murphy, Michael P., Sitti, Metin. 2007. Adhesion of biologically inspired vertical and angled polymer microfiber arrays. *Langmuir* 23:6:3322-3332

Almaviva, S, Botti, S., Cantarini, L., et al. 2012. Trace detection of explosives by Surface Enhanced Raman Spectroscopy. *Optics and Photonics for Counterterrorism, Crime Fighting, and Defence VIII* 8546:Article 854602

Andreou, Chrysafis, Hoonejani, Mehran R., Barmi, Meysam R., et al. 2013. Rapid detection of drug abuse in salvia using surface enhanced Raman spectroscopy and microfluidics. *ACS Nano* 7:8:7157-7164

Beck, Olof, Sandqvist, Soren, Dubbelboer, Ilse, et al. 2011. Detection of delta(9)-tetrahydrocannabinol in exhaled breath collected from cannabis users. *Journal of Analytical Toxicology* 35:8:541-544

Coucke, Line, Massarini, Enrico, Ostijn, Zachery, et al. 2016. Delta(9)-Tetrahydrocannabinol concentration in exhaled breath and physiological effects following cannabis intake – A pilot study using illicit cannabis. *Clinical Biochemistry* 49:13-14:1072-1077

David Day, David Kuntz, Michael Fieldman. 2008. U.S. Patent 7,816,143

Fang, C., Agarwal, A., Ji, H., et al. 2009. Preparation of SERS substrate and its sample-loading method for point-of-use application. *Nanotechnology* 20:40:Article 405604

Fleischmann M, Hendra PJ, McQuillan AJ. 1974. Raman spectra of pyridine adsorbed at a silver electrode. *Chem.Phys.Lett.* 26:163–66

Governing: The States and Localities, “State Marijuana Laws in 2018 Map.” Available from <http://www.governing.com/gov-data/safety-justice/state-marijuana-laws-map-medical-recreational.html>; accessed 16 November 2018

Gustafson, Richard A., Kim, Insook, Stout, Peter R., Huestis, Marilyn A., et al. 2004. Urinary Pharmacokinetics of 11-Nor-9-carboxy- Δ^9 -tetrahydrocannabinol after Controlled Oral Δ^9 -Tetrahydrocannabinol Administration. *Journal of Analytical Toxicology* 28:3:160-167

Haddi, Z., Amari, A., Alami, H., et al. 2011. A portable electronic nose system for the identification of cannabis-based drugs. *Sensors and Actuators B-Chemical* 155:2:456-463

Himes, Sarah K., Scheidweiler, Karl B., Beck, Olof, et al. 2013. Cannabinoids in exhaled breath following controlled administration of smoked cannabis. *Clinical Chemistry* 59:12:1780-1789

Huestis MA, Henningfield JE, Cone EJ. 1992. Blood cannabinoids. I. Absorption of THC and formation of 11-OH-THC and THCCOOH during and after smoking marijuana. *Journal of Analytical Toxicology* 16:5:276-282

Inscore, Frank, Shende, Chetan, Sengupta, Atanu, et al. 2011. Detection of drugs of abuse in saliva by surfaced enhanced Raman spectroscopy (SERS). *Applied Spectroscopy* 65:9:1004-1008

Li, Dongyue, Li, Jing, Xiaofang, Jia, et al. 2013. A novel Au-Ag-Pt three-electrode microchip sensing platform for chromium(VI) determination. *Analytica Chimica Acta* 804:98-103

Li, Mingxiao, Biswas, Souvik, Nantz, Michael H., et al. 2013. A microfabricated preconcentration device for breath analysis. *Sensors and Actuators B-Chemical* 180:SI:130-136

Li, Mingxiao, Huang, Hui, Mao, Haiyang, Li, Li, Zhao, Yang. 2017. Rapid bacteria detection in water based on micro/nano devices. *Transducers* 1570-1572

Liu, Jing, Meng, Guowen, Li, Zhongbo, et al. 2015. Ag-NP@Ge-nanotaper/Si-micropillar ordered arrays as ultrasensitive and uniform surface enhanced Raman scattering substrates. *Nanoscale* 7:43:18218-18224

Madou, Marc J. 2011. *Fundamentals of Microfabrication and Nanotechnology Volume II*. Boca Raton: CRC Press.

Miller, Kane, Li, Mingxiao, Walsh, Kevin M., et al. 2013. The effects of DRIE operational parameters on vertically aligned micropillar arrays. *Microengineering* 23:3:Article 035039

Mohsen, Yehya, Gharbi, Nasser, Lenouvel, Audrey, et al. 2014. Detection of delta(9)-tetrahydrocannabinol, methamphetamine and amphetamine in air at low ppb level using a Field Asymmetric Ion Mobility Spectrometry microchip sensor. *28th European Conference on Solid-State Transducers (Euroensors 2014)* 87:536-539

Nie, Shuming, Emory, Steven R. 1997. Probing single molecules and single nanoparticles by surface-enhanced Raman scattering. *Science* 275:5303:1102-1106

Peng, KG, Yan, YJ, Gao, SP, et al. 2002. Synthesis of large-area silicon nanowire arrays via self-assembling nanoelectrochemistry. *Advanced Materials* 14:16:1164-1167

Peng, KQ, Xu, Y, Wu, Y, et al. 2005. Aligned single-crystalline Si nanowire arrays for photovoltaic applications. *Small* 1:11:1062-1067

PubChem Compound Database, National Center for Biotechnology Information. *Dronabinol*. Available from <https://pubchem.ncbi.nlm.nih.gov/compound/16078#section=Absorption-Distribution-and-Excretion>; accessed 1 April 2017

Quang, Ly Xuan, Lim, Chaesung, Seong, Gi Hun, et al. 2008. A portable surface-enhanced Raman scattering sensor integrated with a lab-on-a-chip for field analysis. *Lab On A Chip* 8:12:2214-2219

Rae Ellen Bichell, "Scientists Still Seek A Reliable DUI Test For Marijuana." *National Public Radio, Inc.*, 30 June 2017, available from <https://www.npr.org/sections/health-shots/2017/07/30/523004450/scientists-still-seek-a-reliable-dui-test-for-marijuana>; accessed 1 November 2017.

Semrock: Idex Health, "Surface-Enhanced Raman Scattering (SERS)." Available from <https://www.semrock.com/surface-enhanced-raman-scattering-sers.aspx>; accessed 16 November 2018

Shao, Ming-Wang, Zhang, Ming-Liang, Wong, Ning-Bew, et al. 2008. Ag-modified silicon nanowires substrate for ultrasensitive surface-enhanced Raman spectroscopy. *Applied Physics Letters* 93:23:Article 233118

Stiles, Paul L., Dieringer, Jon A., Shah, Nilam C., and Van Duyne, Richard P. 2008. Surface-Enhanced Raman Spectroscopy. *Annual Review of Analytical Chemistry*. 1:601-626

U.S. National Library of Medicine, National Institute of Health. *Dronabinol- dronabinol capsule*. Available from <https://dailymed.nlm.nih.gov/dailymed/drugInfo.cfm?setid=68b4168b-5782-4e68-a25a-5b4e4408dbce>; accessed 1 April 2017

Wlodkowic, Donald, Cooper, Jonathan M. 2010. Tumors on chips: oncology meets microfluidics. *Current Opinion in Chemical Biology* 14:5:556-567

Yüksel, Sezin, Schwenke, Almut M., Soliveri, Guido, et al. 2016. Trace detection of tetrahydrocannabinol (THC) with a SERS-based capillary prepared by the in situ microwave synthesis of AgNPs. *Analytical Chimica Acta* 939:93-100

VITA

Jack Thomas Lockard was born June 26, 1995 in Louisville, Kentucky. After attending The Governor's Scholar Program of Kentucky, he went to the University of Louisville and was awarded a Trustees' Scholarship. Due to his love of chemistry instilled by his high school chemistry teacher, Mrs. Alice Hall, he elected to pursue chemical engineering as his major. During his senior year, Jack enrolled in Dr. Xiao An-Fu's Chemical & Biological Microsystems course. The class fascinated him and prompted him to pursue the thesis route for his Master of Engineering in Chemical Engineering. He received his Bachelor's degree in April of 2017 and immediately began pursuing his Master's. In July of 2018, he accepted a position as a process engineer at AGC Automotive Americas in Elizabethtown, Kentucky, while finishing work on his Master's thesis.